 CMC, vol.52, no.2, pp.73-103, 2016

Three-Dimensional Static Analysis of Nanoplates and Graphene Sheets by Using Eringen's Nonlocal Elasticity Theory and the Perturbation Method

Chih-Ping Wu[1,2], **Wei-Chen Li**[1]

Abstract: A three-dimensional (3D) asymptotic theory is reformulated for the static analysis of simply-supported, isotropic and orthotropic single-layered nanoplates and graphene sheets (GSs), in which Eringen's nonlocal elasticity theory is used to capture the small length scale effect on the static behaviors of these. The perturbation method is used to expand the 3D nonlocal elasticity problems as a series of two-dimensional (2D) nonlocal plate problems, the governing equations of which for various order problems retain the same differential operators as those of the nonlocal classical plate theory (CST), although with different nonhomogeneous terms. Expanding the primary field variables of each order as the double Fourier series functions in the in-plane directions, we can obtain the Navier solutions of the leading-order problem, and the higher-order modifications can then be determined in a hierarchic and consistent manner. Some benchmark solutions for the static analysis of isotropic and orthotropic nanoplates and GSs subjected to sinusoidally and uniformly distributed loads are given to demonstrate the performance of the 3D nonlocal asymptotic theory.

Keywords: Eringen's nonlocal elasticity theory, graphene sheets, nanoplates, static, the perturbation method, three-dimensional nonlocal elasticity.

1 Introduction

The fields of nanoscience and nanotechnology, as well as their application in advanced industries, have developed significantly since carbon nanotubes (CNTs) [Iijima (1991)] and graphene sheets (GSs) [Novoselov, Geim, Morozov, Jiang, Zhang, Dubonos, Grigorieva, and Firsov (2004)] were first discovered. These two nanoscale materials, possessing excellent mechanical, chemical, thermal and electrical material properties, have thus been introduced in a variety of poten-

[1] Department of Civil Engineering, National Cheng Kung University, Tainan 70101, Taiwan, ROC
[2] Corresponding author. Fax: +886-6-2370804 E-mail address: cpwu@mail.ncku.edu.tw

tial applications to both micro- and nano-electro-mechanical systems (MEMs and NEMs) [Brischetto and Carrera (2012a, 2012b); Wang (2004); Wang and Liew (2008)]. They have also been combined with polymer materials to form CNT- and GS-reinforced composite structures, with studies showing that they are capable of optimally arranging their distributions in the interior domains of these to obtain various extreme characteristics that can be used in structural designs [Coleman, Khan, Blau, and Gun'ko (2006); Esawi and Farag (2007); Li, Thostenson, and Chou (2008); Liew, Lei, and Zhang (2015); Ramaratnam and Jalili (2006)]. A comprehensive literature survey with regard to the application of nonlocal elastic models in the modeling of CNTs and GSs has been undertaken by Arash and Wang (2012).

Because GSs have being widely used in MEMs, NEMS and other forms of nanotechnology, it is important to be able to accurately analyze their structural behaviors in order to extend their lifetimes and enhance their performance. This paper thus focuses on a literature survey related to the mechanical analysis of nanoplates and GSs using Eringen's nonlocal elasticity theory (ENET) [Eringen (1972, 2002); Eringen and Edelen (1972)].

Some two-dimensional (2D) nonlocal plate theories have been used to investigate the mechanical behavior of nanoplates and GSs. By using the ENET, Aghababaei and Reddy (2009) reformulated Reddy's third-order shear deformation plate theory (TSDPT) for macroscale plates [Reddy (1984); Reddy and Phan (1985)] to obtain its counterpart for nanoplates and GSs. The TSDPT were applied to examine the bending and vibration behavior of nanoplates, in which the Navier solutions of the stress and displacement components and natural frequency parameters of simply-supported, nanoplates were presented. The small size effects on the static and vibration behavior of the nanoplates, and comparisons between their solutions and those obtained by using the nonlocal first-order shear deformation plate theory (FSDPT) and nonlocal classical plate theory (CPT), were undertaken. The nonlocal TSDPT was used by Hosseini-Hashemi, Kermajani, and Nazemnezhad (2015) to study the buckling and free vibration of rectangular nanoplates, in which the Levy solutions of critical loads and frequency parameters of rectangular nanoplates were presented. Based on the nonlocal CPT, Kitipornchai, He and Liew (2005) and Liew, He, and Kitipornchai (2006) investigated the free vibration behavior of multilayered GSs without and with being embedded in an elastic medium, respectively. By accounting for the van der Waals interactions between different GSs and Winkler's foundation model, the corresponding set of explicit formulas were derived to predict the natural frequency parameters and their associated vibration modes of double- and triple-layered GSs. In conjunction with the ENET and von Karman nonlinear strains, Reddy (2010) developed the nonlinear formulations of the non-

local FSDPT and CPT for the static analysis of nanoplates. Based on the nonlocal TSDPT, Arani and Jalaei (2015) analytically investigated the static and dynamic responses of simply-supported, single-layered GSs embedded in an elastic medium under uniform and sinusoidal loads, in which a visco-Pasternak foundation model was used to simulate the interaction between the GSs and their surrounding medium. Pradhan and Phadikar (2009) presented the nonlocal FSDPT and nonlocal CPT for the vibration analysis of nanoplates and GSs by reformulating its local counterparts and using the ENET. The nonlocal FSDPT and CPT were also extended to the analysis of double-layered nanoplates, in which some effects on natural frequency parameters of the nanoplate were investigated, such as the nonlocal parameter, aspect ratio, Young's modulus of the nanoplate and stiffness of Winkler foundation effects. The CPT was reformulated by Pradhan and Kumar (2011) for the vibration analysis of single-layered orthotropic GSs with various boundary conditions by using the differential quadrature (DQ) method and ENET, in which the effects of small length scale, aspect ratio and boundary conditions on the vibration characteristics of these were examined. The nonlocal CPT was also used by Shen, Shen, and Zhang (2010) for the nonlinear vibration analysis of single-layered GSs in thermal environments. Duan and Wang (2007) presented the exact solutions for the axisymmetric bending analysis of nanoscale circular plates on the basis of the nonlocal CPT. It has been shown that the nonlocal solutions of deflections, moments and shear forces are larger than their counterpart local solutions. Wang and Li (2012) developed the nonlocal Mindlin and Kirchhoff plate theories to study the static behavior of nanoplates embedded in elastic matrix by accounting for the small length scale effect. Wen, Huang, and Aliabadi (2013) developed a 2D local boundary integral method for the nonlocal elasticity theory with 2D Eringen's model. Based on the nonlocal refined sinusoidal shear deformation plate theory (SSDPT), Thai (2012); Thai and Vo (2012) and Thai, Vo, Nguyen, and Lee (2014) presented the analytical solutions for the bending, buckling and vibration problems of nanobeams and nanoplates, and concluded that the small scale and shear deformation effects are significant for the structural behaviors of these when the nanobeams and nanoplates become thicker. Zenkour and Sobhy (2013) and Alzahrani, Zenkour, and Sobhy (2013) applied the refined SSDPT to the thermal buckling and hygro-thermo-mechanical bending analyses of nanoplates embedded in an elastic medium, respectively, in which the interaction between the nanoplate and its surrounding medium was modelled as a Winkler-Pasternak foundation. Li and Pan (2016) developed an SSDPT for the bending analysis of simply-supported, piezoelectric nanoplates considering the surface effects.

Some studies have carried out three-dimensional (3D) analyses of the static behaviors and dynamic responses of simply-supported, nanoplates and GSs. For exam-

ples, Wu, Chiu, and Wang (2008) classified the 3D exact approaches for simply-supported macrostructures available in the literature into four different categories, namely, the state space, series expansion, Pagano and perturbation methods. Among these, only the state space method was successfully extended to the 3D analysis of nanostructures. Within the framework of 3D nonlocal elasticity theory, Alibeigloo and Zanoosi (2013) and Alibeigloo (2011) analyzed the static and free vibration behavior of simply-supported, rectangular GSs, respectively, by using the state space method in the thickness direction and Fourier series in the in-plane directions. The effects of the nonlocal parameter, aspect ratio and half-wave numbers on the deformations and stresses induced in the single-layered nanoplates and their natural frequency parameters were examined. The state space method was also extensively applied to the 3D free vibration analysis of multi-layered GSs embedded in an elastic medium by Alibeigloo (2012). By using the cylindrical coordinate system, Brischetto (2014) reformulated the 3D nonlocal state space equations for the free vibration behavior of simply-supported, single-layered CNTs. The natural frequency parameters and their corresponding vibration modes were obtained by using the state space method. The 3D nonlocal solutions were compared with the one-dimensional (1D) nonlocal beam ones in order to show the limitations of 1D beam models. Brischetto, Tornabene, Fantuzzi, and Bacciocchi (2015) presented a comparative study with regard to the free vibration behavior of single- and double-walled CNTs by using the refined 2D and exact 3D shell models, in which the van der Waals interactions between the two cylinders were included. Based on the nonlocal elasticity theory, Ghavanloo and Fazelzadeh (2013) investigated the radial vibration of nanoscale spherical shells. It has been concluded that the small length scale effect on the frequency parameters of nanoshells is significant. Ansari, Shojaei, Shahabodini, and Bazdid-Vahdati (2015) studied the 3D bending and vibration analyses of functionally graded (FG) nanoplates with various boundary conditions. In their formulation, Hamilton's principle was used to derive the motion of equations of the nanoplate, the material properties of which were assumed to vary through the thickness coordinate with power-law and exponential distributions, and then the variational differential quadrature method was used to obtain the 3D nonlocal solutions for the bending and free vibration problems of FG nanoplates.

Due to the mathematical complexity of 3D nonlocal elasticity theories of nanoplates and GSs, there are relatively few papers related to the 3D mechanical behavior of these available in the literature, when compared to the number of papers that examine those of macrostructures. To the best of the authors' knowledge, the perturbation method [Nayfeh (1993)] has never been applied to the 3D mechanical analysis of nanoplates and GSs, even though it has been successfully applied to that of macrostructures, such as laminated composite structures [Wu and Chiu (2002);

Wu, Tarn, and Chi (1996a, 1996b); Wu, Tarn, and Chen (1997)] and FG elastic/piezoelectric ones [Wu and Syu (2007); Wu and Tsai (2004)]. An asymptotic theory is thus developed in this work for the 3D static analysis of simply-supported, rectangular nanoplates and GSs by using the perturbation method combined with Eringen's nonlocal elasticity theory. Using direct elimination, we first reduce the fifteen partially differential equations (PDEs) of the 3D nonlocal elasticity theory to six PDEs in terms of three displacement components and three transverse shear and normal stress ones. Through the mathematical manipulation of nondimensionalization, asymptotic expansion and successive integration, we finally obtain recurrent sets of nonlocal governing equations for various order problems. The nonlocal CPT is derived as a first-order approximation of the 3D nonlocal elasticity theory, and the nonlocal governing equations for higher-order problems retain the same differential operators as those of the nonlocal CPT, although with different nonhomogeneous terms. Expanding the primary field variables of each order as the Fourier series functions in the in-plane directions, we can obtain the Navier solutions of the leading-order problem, and the higher-order modifications can then be determined in a systematic manner. The asymptotic approach is different from methods based on the 2D nonlocal advanced and refined theories. In the latter, a set of kinetic and kinematic models is assumed *a priori*, and this has to be replaced by using a much higher-order model when the accuracy of the original model needs to be improved, and thus the formulation must be totally changed. In contrast, in the former the leading-order solutions are identical to the nonlocal CPT ones, and the accuracy can be improved by performing higher-order modifications and without changing the whole formulation. Moreover, the 3D asymptotic solutions will approach the exact 3D nonlocal elasticity solutions order by order.

Some benchmark solutions for the static analysis of simply-supported, isotropic and orthotropic macro- and nano-plates subjected to sinusoidally- and uniformly-distributed loads are given to demonstrate the performance of the 3D nonlocal asymptotic theory, in which the nonlocal parameter (μ) is taken to be zero for the macroplates and positive values, which should be less than 4 nm^2 [Wang and Wang (2007)], for nanoplates and GSs. The 3D results for the nanoplates and GSs may provide a reference for assessing those obtained using the 2D advanced and refined nanoplate theories. Moreover, the effects of the nonlocal parameter, aspect ratio, and in-plane dimension-to-thickness ratio on the stress and displacement components induced in the loaded nanoplates and GSs are also examined.

2 Basic equations of 3D nonlocal elasticity theory

As shown in Fig. 1, we consider a simply-supported elastic nanoplate (or GS), subjected to a sinusoidally distributed load. A set of Cartesian coordinates (x, y and

z) is located at the mid-plane of the plate, the thickness and in-plane dimension of which are denoted as H and (L_x x L_y), respectively.

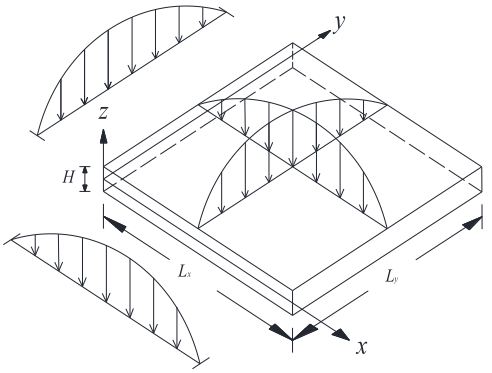

Figure 1: Geometric parameters and configuration of a nanoplate (or GS) under the sinusoidally distributed load.

The main difference between the local and nonlocal elasticity theories is in their descriptions of the constitutive relation of a Hookean solid. In the former, the stress components induced at a particular material point of the loaded elastic body depend only on the strain components induced at that point, while in the latter, these will depend on the strain components induced at all the material points of the continuum, due to the small length scale effect. According to Eringen (1972, 2002) and Eringen and Edelen (1972), the nonlocal constitutive behavior of an elastic body can be written as

$$\sigma_{ij}(\mathbf{x}) = \int \alpha\left(\left|\mathbf{x}-\mathbf{x}'\right|,\tau\right) C_{ijkl}\varepsilon_{kl}\left(\mathbf{x}'\right) dV\left(\mathbf{x}'\right), \quad \forall \mathbf{x} \in V, \tag{1}$$

where the elastic modulus tensor of classical isotropic elasticity is defined as C_{ijkl}, and stress and strain tensors are σ_{ij} and ε_{kl}, respectively. The nonlocal modulus or attenuation function, which incorporates the constitutive equations into the nonlocal effect at the reference point $\mathbf{x}$ produced by local strain at the source $\mathbf{x}'$, is defined as $\alpha(|\mathbf{x}-\mathbf{x}'|,\tau)$, in which the symbol $|\mathbf{x}-\mathbf{x}'|$ is the Euclidean distance. $\tau = e_0 a/l$, in which e_0 is a constant appropriate to each material, a is an internal characteristic length (e.g., length of C-C bond, lattice parameter, or granular distance), and l is an external characteristic length (e.g., crack length or wavelength). The value of e_0 needs to be determined from experiments or by matching the dispersion curves of plane waves with those of atomic lattice dynamics [Wang (2005)].

The integral-partial differential equations of Eq. (1) can be further reduced to singular partial differential equations of a special class of physically admissible kernel,

as follows:

$$\left(1-\mu\nabla^2\right)\sigma_{ij}=C_{ijkl}\varepsilon_{kl}, \tag{2}$$

where μ is the nonlocal parameter, and $\mu=(e_0a)^2$, and $e_0a<2.0$ nm for a single-walled CNT [Wang and Wang (2007)]. ∇^2 is the Laplacian operator, in which $\nabla^2=(\partial_{xx}+\partial_{yy}+\partial_{zz})$ is used for a 3D nonlocal elastic problem, while $\nabla^2=(\partial_{xx}+\partial_{yy})$ and $\nabla^2=\partial_{xx}$ for the 2D and 1D nonlocal elastic ones, and $\partial_{xx}=\partial^2/\partial x^2$.

According to Eringen's elasticity theory, the linear constitutive equations valid for the symmetrical class of elastic materials are given by

$$\left(1-\mu\nabla^2\right)\begin{Bmatrix}\sigma_x\\ \sigma_y\\ \sigma_z\\ \tau_{yz}\\ \tau_{xz}\\ \tau_{xy}\end{Bmatrix}=\begin{bmatrix}c_{11} & c_{12} & c_{13} & 0 & 0 & 0\\ c_{12} & c_{22} & c_{23} & 0 & 0 & 0\\ c_{13} & c_{23} & c_{33} & 0 & 0 & 0\\ 0 & 0 & 0 & c_{44} & 0 & 0\\ 0 & 0 & 0 & 0 & c_{55} & 0\\ 0 & 0 & 0 & 0 & 0 & c_{66}\end{bmatrix}\begin{Bmatrix}\varepsilon_x\\ \varepsilon_y\\ \varepsilon_z\\ \gamma_{yz}\\ \gamma_{xz}\\ \gamma_{xy}\end{Bmatrix} \tag{3}$$

where $(\varepsilon_x,\varepsilon_y,\varepsilon_z,\gamma_{xz},\gamma_{yz},\gamma_{xy})$ denote the strain components. $(\sigma_x^{nl},\sigma_y^{nl},\sigma_z^{nl},\tau_{xz}^{nl},\tau_{yz}^{nl},\tau_{xy}^{nl})$ and $(\sigma_x,\sigma_y,\sigma_z,\tau_{xz},\tau_{yz},\tau_{xy})$ are defined as the nonlocal and local stress components, respectively, in which $(\sigma_x^{nl},\sigma_y^{nl},\sigma_z^{nl},\tau_{xz}^{nl},\tau_{yz}^{nl},\tau_{xy}^{nl})=(1-\mu\nabla^2)(\sigma_x,\sigma_y,\sigma_z,\tau_{xz},\tau_{yz},\tau_{xy})$. c_{ij} $(i,\ j=1\text{–}6)$ are the elastic coefficients relative to the geometrical axes of the plate. For an isotropic material nanoplate the coefficients c_{ij} will be reduced to $c_{11}=c_{22}=c_{33}=[(1-\upsilon)\,E/(1+\upsilon)\,(1-2\upsilon)]$, $c_{12}=c_{13}=c_{23}=[\upsilon E/(1+\upsilon)\,(1-2\upsilon)]$ and $c_{44}=c_{55}=c_{66}=[E/2\,(1+\upsilon)]$, in which E and υ are the Young's modulus and Poisson's ratio, respectively.

The kinematic equations in terms of the Cartesian coordinates are

$$\varepsilon_x=\frac{\partial u_x}{\partial x}, \tag{4a}$$

$$\varepsilon_y=\frac{\partial u_y}{\partial y} \tag{4b}$$

$$\varepsilon_r=\frac{\partial u_z}{\partial z}, \tag{4c}$$

$$\gamma_{xz}=\frac{\partial u_x}{\partial z}+\frac{\partial u_z}{\partial x}, \tag{4d}$$

$$\gamma_{yz}=\frac{\partial u_y}{\partial z}+\frac{\partial u_z}{\partial y}, \tag{4e}$$

$$\gamma_{xy}=\frac{\partial u_x}{\partial y}+\frac{\partial u_y}{\partial x}. \tag{4f}$$

in which u_x, u_y and u_z are the displacement components.

The stress equilibrium equations of an elastic body without accounting for body forces are given by

$$\frac{\partial \sigma_x}{\partial x} + \frac{\partial \tau_{xy}}{\partial y} + \frac{\partial \tau_{xz}}{\partial z} = 0, \tag{5}$$

$$\frac{\partial \tau_{xy}}{\partial x} + \frac{\partial \sigma_y}{\partial y} + \frac{\partial \tau_{yz}}{\partial z} = 0, \tag{6}$$

$$\frac{\partial \tau_{xz}}{\partial x} + \frac{\partial \tau_{yz}}{\partial y} + \frac{\partial \sigma_z}{\partial z} = 0. \tag{7}$$

The boundary conditions of the problem are specified, as follows:

On the top and bottom surfaces the transverse loads are given by

$$[\tau_{xz} \;\; \tau_{yz} \;\; \sigma_z] = \left[0 \;\; 0 \;\; -\bar{q}_z^{\pm}\right] \;\; \text{on} \;\; z = \pm h, \tag{8}$$

where h denotes one-half of the total thickness (H), and the positive directions of $\bar{q}_z^+$ and $\bar{q}_z^-$ are defined to be downward and upward, respectively.

The edge boundary conditions of the plate are considered as simply-supported ones, and are given as follows:

At the edges ($x = 0$ and $x = L_x$), the boundary conditions are

$$\sigma_x = u_y = u_z = 0, \tag{9a}$$

At the edges ($y = 0$ and $y = L_y$), the boundary conditions are

$$\sigma_y = u_x = u_z = 0. \tag{9b}$$

3 Nondimensionalization

A set of dimensionless coordinates and elastic field variables is defined, as follows:

$$x_1 = x/L, \tag{10a}$$
$$x_2 = y/L, \tag{10b}$$
$$x_3 = z/(L \in), \tag{10c}$$
$$u_1 = u_x/(L \in), \tag{10d}$$
$$u_2 = u_y/(L \in), \tag{10e}$$
$$u_3 = u_z/L, \tag{10f}$$
$$\sigma_1 = \sigma_x/(Q \in), \tag{10g}$$

$$\sigma_2 = \sigma_y/(Q\in), \tag{10h}$$
$$\tau_{12} = \tau_{xy}/(Q\in), \tag{10i}$$
$$\tau_{13} = \tau_{xz}/\left(Q\in^2\right), \tag{10j}$$
$$\tau_{23} = \tau_{yz}/\left(Q\in^2\right), \tag{10k}$$
$$\sigma_3 = \sigma_z/\left(Q\in^3\right), \tag{10l}$$
$$\bar{\mu}_1 = \mu/L^2, \tag{10m}$$
$$\bar{\mu}_2 = \mu/\left(L^2\in^4\right), \tag{10n}$$

where $\in = h/L$. L and Q denote the reference length and elastic modulus, and these are given as $L = \sqrt{L_x L_y}$ and $Q = c_{33}$ in this work.

As we previously listed in Eqs. (3)–(7), there are fifteen basic equations of 3D nonlocal elasticity theory for the static analysis of nanoplates and GSs, subjected to mechanical loads. In order to make the formulation suitable for mathematical treatment, we eliminate the in-plane stress $(\sigma_x, \sigma_y, \tau_{xy})$ and strain $(\varepsilon_x, \varepsilon_y, \varepsilon_z, \gamma_{xz}, \gamma_{yz}, \gamma_{xy})$ components from Eqs. (3)– (7), introduce Eq. (10) in the resulting equations, and then express the 3D basic equations in terms of the dimensionless forms of displacement (u_1, u_2, u_3) and transverse stress $(\tau_{13}, \tau_{23}, \sigma_3)$ components, as follows:

$$u_{3,3} = -\in^2 \mathbf{L}_1 \mathbf{u} + \in^4 \tilde{c}_{33}^{-1} \left[1 - \bar{\mu}_1 \partial_{11} - \bar{\mu}_1 \partial_{22}\right] \sigma_3 - \in^6 \left(\tilde{c}_{33}^{-1} \bar{\mu}_2 \partial_{33}\right) \sigma_3, \tag{11}$$

$$\mathbf{u}_{,3} = -\mathbf{D}u_3 + \in^2 \mathbf{S}\left[1 - \bar{\mu}_1\partial_{11} - \bar{\mu}_1\partial_{22}\right]\sigma_s - \in^4 \mathbf{S}\left(\bar{\mu}_2\partial_{33}\right)\sigma_s, \tag{12}$$

$$\left[\left(1 - \bar{\mu}_1\partial_{11} - \bar{\mu}_1\partial_{22}\right)\sigma_s\right]_{,3} = -\mathbf{L}_2\mathbf{u} + \in^2 \left(\bar{\mu}_2\partial_{333}\right)\sigma_s - \in^2 \mathbf{L}_3 \left(1 - \bar{\mu}_1\partial_{11} - \bar{\mu}_1\partial_{22}\right)\sigma_3 + \in^4 \mathbf{L}_3 \left(\bar{\mu}_2\partial_{33}\right)\sigma_3, \tag{13}$$

$$\left[\left(1 - \bar{\mu}_1\partial_{11} - \bar{\mu}_1\partial_{22}\right)\sigma_3\right]_{,3} = -\mathbf{D}^T \left[\left(1 - \bar{\mu}_1\partial_{11} - \bar{\mu}_1\partial_{22}\right)\sigma_s\right], \tag{14}$$

where

$$\mathbf{u} = \begin{Bmatrix} u_1 \\ u_2 \end{Bmatrix}, \quad \mathbf{D} = \begin{Bmatrix} \partial_1 \\ \partial_2 \end{Bmatrix}, \quad \mathbf{S} = \begin{bmatrix} \left(\tilde{c}_{55}^{-1}\right) & 0 \\ 0 & \left(\tilde{c}_{44}^{-1}\right) \end{bmatrix}, \quad \sigma_s = \begin{Bmatrix} \tau_{13} \\ \tau_{23} \end{Bmatrix},$$

$$\mathbf{L}_1 = \begin{bmatrix} \tilde{l}_{31} & \tilde{l}_{32} \end{bmatrix}, \quad \mathbf{L}_2 = \begin{bmatrix} \tilde{l}_{41} & \tilde{l}_{42} \\ \tilde{l}_{42} & \tilde{l}_{52} \end{bmatrix}, \quad \mathbf{L}_3 = \begin{bmatrix} \tilde{l}_{31} \\ \tilde{l}_{32} \end{bmatrix},$$

$$\tilde{l}_{31} = \tilde{c}_{13}\partial_1, \quad \tilde{l}_{32} = \tilde{c}_{23}\partial_2, \quad \tilde{l}_{41} = \tilde{Q}_{11}\partial_{11} + \tilde{Q}_{66}\partial_{22}, \quad \tilde{l}_{42} = \left(\tilde{Q}_{12} + \tilde{Q}_{66}\right)\partial_{12},$$

$$\tilde{l}_{52} = \tilde{Q}_{66}\partial_{11} + \tilde{Q}_{22}\partial_{22}, \quad \tilde{c}_{i3} = c_{i3}/c_{33} \quad (i = 1 \text{ and } 2),$$

$$\tilde{c}_{kk} = c_{kk}/Q\,(k = 3-5), \quad \tilde{Q}_{ij} = Q_{ij}/Q, \quad Q_{ij} = c_{ij} - (c_{i3}c_{j3}/c_{33})\,(i = 1,2 \text{ and } 6).$$

Following a similar derivation process, we rewrite the in-surface stresses in the dimensionless form, as follows:

$$(1-\bar{\mu}_1\partial_{11}-\bar{\mu}_1\partial_{22})\,\sigma_p=\mathbf{B}_1\mathbf{u}+\in^2(\bar{\mu}_2\partial_{33})\,\sigma_p+\in^2\mathbf{B}_2\,(1-\bar{\mu}_1\partial_{11}-\bar{\mu}_1\partial_{22})\,\sigma_3 \\ -\in^4\mathbf{B}_2\,(\bar{\mu}_2\partial_{33})\,\sigma_3, \tag{15}$$

where

$$\sigma_p=\begin{Bmatrix}\sigma_1\\ \sigma_2\\ \tau_{12}\end{Bmatrix},\quad \mathbf{B}_1=\begin{bmatrix}\tilde{Q}_{11}\partial_1 & \tilde{Q}_{12}\partial_2\\ \tilde{Q}_{12}\partial_1 & \tilde{Q}_{22}\partial_2\\ \tilde{Q}_{66}\partial_2 & \tilde{Q}_{66}\partial_1\end{bmatrix},\quad \mathbf{B}_2=\begin{bmatrix}\tilde{c}_{13}\\ \tilde{c}_{23}\\ 0\end{bmatrix}.$$

The dimensionless forms of the boundary conditions of the problem are specified as follows:

On the top and bottom surfaces the transverse loads are given by

$$[\tau_{13}\quad \tau_{23}\quad \sigma_3]=\left[0\quad 0\quad -\bar{q}_3^{\pm}\right]\quad \text{on}\quad x_3=\pm 1, \tag{16}$$

in which $\bar{q}_3^{\pm}=\bar{q}_z^{\pm}/\left(Q\in^3\right)$.

At the edges ($x_1=0$ and $x_1=L_x/L$), the boundary conditions are

$$\sigma_1=u_2=u_3=0 \tag{17a}$$

At the edges ($x_2=0$ and $x_2=L_y/L$), the boundary conditions are

$$\sigma_2=u_1=u_3=0 \tag{17b}$$

4 Asymptotic expansion

Because Eqs. (11)–(15) contain terms involving only even powers of $\in$, we asymptotically expand the field variables in the powers $\in^2$, as given by

$$f=f^{(0)}(x_1,x_2,x_3)+\in^2 f^{(1)}(x_1,x_2,x_3)+\in^4 f^{(2)}(x_1,x_2,x_3)+\cdots. \tag{18}$$

Substituting Eq. (18) into Eqs. (11)–(15) and collecting coefficients of equal powers of $\in$, we obtain the following sets of recurrence equations.

Order $\in^0$:

$$u_3^{(0)},_3=0, \tag{19}$$

$$\mathbf{u}^{(0)},_3=-\mathbf{D}u_3^{(0)}, \tag{20}$$

$$\left[(1-\bar{\mu}_1\partial_{11}-\bar{\mu}_1\partial_{22})\,\sigma_s^{(0)}\right],_3=-\mathbf{L}_2\mathbf{u}^{(0)}, \tag{21}$$

$$\left[\left(1-\bar{\mu}_1\partial_{11}-\bar{\mu}_1\partial_{22}\right)\sigma_3^{(0)}\right],_3=-\mathbf{D}^T\left[\left(1-\bar{\mu}_1\partial_{11}-\bar{\mu}_1\partial_{22}\right)\sigma_s^{(0)}\right], \tag{22}$$

$$\left(1-\bar{\mu}_1\partial_{11}-\bar{\mu}_1\partial_{22}\right)\sigma_p^{(0)}=\mathbf{B}_1\mathbf{u}^{(0)}, \tag{23}$$

Order $\in^{2k}$ $(k=1,2,3,\ldots)$:

$$u_3^{(k)},_3=-\mathbf{L}_1\mathbf{u}^{(k-1)}+\tilde{c}_{33}^{-1}\left[1-\bar{\mu}_1\partial_{11}-\bar{\mu}_1\partial_{22}\right]\sigma_3^{(k-2)}-\left(\tilde{c}_{33}^{-1}\bar{\mu}_2\partial_{33}\right)\sigma_3^{(k-3)}, \tag{24}$$

$$\mathbf{u}^{(k)},_3=-\mathbf{D}u_3^{(k)}+\mathbf{S}\left[1-\bar{\mu}_1\partial_{11}-\bar{\mu}_1\partial_{22}\right]\sigma_s^{(k-1)}-\mathbf{S}\left(\bar{\mu}_2\partial_{33}\right)\sigma_s^{(k-2)}, \tag{25}$$

$$\begin{aligned}&\left[\left(1-\bar{\mu}_1\partial_{11}-\bar{\mu}_1\partial_{22}\right)\sigma_s^{(k)}\right],_3=-\mathbf{L}_2\mathbf{u}^{(k)}+\left(\bar{\mu}_2\partial_{333}\right)\sigma_s^{(k-1)}\\&-\mathbf{L}_3\left(1-\bar{\mu}_1\partial_{11}-\bar{\mu}_1\partial_{22}\right)\sigma_3^{(k-1)}+\mathbf{L}_3\left(\bar{\mu}_2\partial_{33}\right)\sigma_3^{(k-2)},\end{aligned} \tag{26}$$

$$\left[\left(1-\bar{\mu}_1\partial_{11}-\bar{\mu}_1\partial_{22}\right)\sigma_3^{(k)}\right],_3=-\mathbf{D}^T\left[\left(1-\bar{\mu}_1\partial_{11}-\bar{\mu}_1\partial_{22}\right)\sigma_s^{(k)}\right], \tag{27}$$

$$\begin{aligned}\left(1-\bar{\mu}_1\partial_{11}-\bar{\mu}_1\partial_{22}\right)\sigma_p^{(k)}&=\mathbf{B}_1\mathbf{u}^{(k)}+\left(\bar{\mu}_2\partial_{33}\right)\sigma_p^{(k-1)}+\mathbf{B}_2\left(1-\bar{\mu}_1\partial_{11}-\bar{\mu}_1\partial_{22}\right)\sigma_3^{(k-1)}\\&-\mathbf{B}_2\left(\bar{\mu}_2\partial_{33}\right)\sigma_3^{(k-2)}.\end{aligned} \tag{28}$$

The boundary conditions for various order problems are specified, as follows:

On the top and bottom surfaces the transverse loads are

Order $\in^0$,

$$\left[\tau_{13}^{(0)}\quad\tau_{23}^{(0)}\quad\sigma_3^{(0)}\right]=\left[0\quad 0\quad-\bar{q}_3^{\pm}\right]\quad\text{on}\quad x_3=\pm 1, \tag{29a}$$

Order $\in^{2k}$ $(k=1,2,3,\text{etc})$,

$$\left[\tau_{13}^{(k)}\quad\tau_{23}^{(k)}\quad\sigma_3^{(k)}\right]=[0\quad 0\quad 0]\quad\text{on}\quad x_3=\pm 1. \tag{29b}$$

Along the edges ($x_1=0$ and $x_1=L_x/L$), the boundary conditions are given, as follows:

order $\in^{2k}$ $(k=0,1,2,3,\text{etc})$,

$$\sigma_1^{(k)}=u_2^{(k)}=u_3^{(k)}=0; \tag{30a}$$

Along the edges ($x_2=0$ and $x_2=L_y/L$), the boundary conditions are given as follows:

order $\in^{2k}$ $(k=0,1,2,3,\text{etc})$,

$$\sigma_2^{(k)}=u_1^{(k)}=u_3^{(k)}=0. \tag{30b}$$

5 Asymptotic integration

5.1 The leading-order problem

We examine the sets of asymptotic equations and find that the present analysis can be carried out by integrating these through the thickness direction. We thus integrate Eqs. (19) and (20) to obtain

$$u_3^{(0)} = u_3^0(x_1,x_2), \tag{31}$$

$$\mathbf{u}^{(0)} = \mathbf{u}^0 - x_3\mathbf{D}u_3^0, \tag{32}$$

where u_3^0 and $\mathbf{u}^0 = \begin{bmatrix} u_1^0(x_1,x_2) & u_2^0(x_1,x_2) \end{bmatrix}^T$ represent the displacement components on the mid-plane, and these are also of the Kirchhoff-Love type in CPT.

With the lateral boundary conditions on x_3 =-1 given in Eq. (29a), we then proceed to integrate Eqs. (21) and (22), which yields

$$\left(1-\bar{\mu}_1\partial_{11}-\bar{\mu}_1\partial_{22}\right)\sigma_s^{(0)} = -\int_{-1}^{x_3}\left[\mathbf{L}_2\left(\mathbf{u}^0-\eta\mathbf{D}u_3^0\right)\right]d\eta, \tag{33}$$

$$\left(1-\bar{\mu}_1\partial_{11}-\bar{\mu}_1\partial_{22}\right)\left(\sigma_3^{(0)}+\bar{q}_3^-\right) = \int_{-1}^{x_3}(x_3-\eta)\mathbf{D}^T\left[\mathbf{L}_2\left(\mathbf{u}^0-\eta\mathbf{D}u_3^0\right)\right]d\eta, \tag{34}$$

Imposing the remaining lateral boundary conditions on $x_3 = 1$ given in Eq. (29b) in Eqs. (33) and (34), we obtain

$$K_{11}u_1^0 + K_{12}u_2^0 + K_{13}u_3^0 = 0, \tag{35}$$

$$K_{21}u_1^0 + K_{22}u_2^0 + K_{23}u_3^0 = 0, \tag{36}$$

$$K_{31}u_1^0 + K_{32}u_2^0 + K_{33}u_3^0 = -\left(1-\bar{\mu}_1\partial_{11}-\bar{\mu}_1\partial_{22}\right)\left(\bar{q}_3^+-\bar{q}_3^-\right), \tag{37}$$

where

$$K_{11} = -\tilde{A}_{11}\partial_{11} - \tilde{A}_{66}\partial_{22}, \tag{38a}$$
$$K_{12} = -\left(\tilde{A}_{12}+\tilde{A}_{66}\right)\partial_{12}, \tag{38b}$$
$$K_{13} = \tilde{B}_{11}\partial_{111} + \left(\tilde{B}_{12}+2\tilde{B}_{66}\right)\partial_{122}, \tag{38c}$$
$$K_{21} = K_{12}, \tag{38d}$$
$$K_{22} = -\tilde{A}_{66}\partial_{11} - \tilde{A}_{22}\partial_{22}, \tag{38e}$$
$$K_{23} = \left(\tilde{B}_{12}+2\tilde{B}_{66}\right)\partial_{112} + \tilde{B}_{22}\partial_{222}, \tag{38f}$$
$$K_{31} = -K_{13}, \tag{38g}$$
$$K_{32} = -K_{23}, \tag{38h}$$
$$K_{33} = \tilde{D}_{11}\partial_{1111} + \left(2\tilde{D}_{12}+4\tilde{D}_{66}\right)\partial_{1122} + \tilde{D}_{22}\partial_{2222}, \tag{38i}$$

$$\tilde{A}_{ij} = \int_{-1}^{1} \tilde{Q}_{ij} dx_3, \tag{38j}$$

$$\tilde{B}_{ij} = \int_{-1}^{1} x_3 \tilde{Q}_{ij} dz, \tag{38k}$$

$$\tilde{D}_{ij} = \int_{-1}^{1} x_3^2 \tilde{Q}_{ij} dx_3. \tag{38l}$$

In this paper, the edge boundary conditions of the plate are considered as fully simply-supported edges. After the asymptotic process, we thus obtain the edge conditions for the leading order problem, as follows:

$$u_2^0 = 0, u_3^0 = 0, N_1^{(0)} = 0 \text{ and } M_1^{(0)} = 0, \text{ at } x_1 = 0 \text{ and } x_1 = L_x/L, \tag{39a}$$

$$u_1^0 = 0, u_3^0 = 0, N_2^{(0)} = 0 \text{ and } M_2^{(0)} = 0, \text{ at } x_2 = 0 \text{ and } x_2 = L_y/L, \tag{39b}$$

in which $N_i^{(0)} = \int_{-1}^{1} \sigma_i^{(0)} dx_3$, $M_i^{(0)} = \int_{-1}^{1} x_3 \sigma_i^{(0)} dx_3$, and $i = 1$ and 2.

It is noted that Eqs. (35)–(37) are exactly the same as the governing equations of the nonlocal CPT [Pradhan and Kumar (2011); Shen, Shen, and Zhang (2010)], which have thus been derived as a first-order approximation of the 3D nonlocal elasticity theory. Solutions of Eqs. (35)–(37) must be supplemented with the edge boundary conditions given in Eqs. (39a) and (39b) to constitute a well-posed boundary value problem. Once the variables of u_1^0, u_2^0 and u_3^0 are determined, the leading-order solutions of displacements through the plate thickness are given by Eqs. (31) and (32), the transverse shear and normal stresses by Eqs. (33) and (34) and the in-surface stresses by Eq. (23).

5.2 Higher-order problems

Proceeding to order $\in^{2k}$ $(k = 1, 2, 3, \ldots)$ and following the same process as before, we readily obtain

$$u_3^{(k)} = u_3^k(x_1, x_2) + \varphi_{3k}(x_1, x_2, x_3), \tag{40}$$

$$\mathbf{u}^{(\mathrm{k})} = \mathbf{u}^k(x_1, x_2) - x_3 \mathbf{D} u_3^k + \boldsymbol{\varphi}^k(x_1, x_2, x_3), \tag{41}$$

$$(1 - \bar{\mu}_1 \partial_{11} - \bar{\mu}_1 \partial_{22}) \sigma_s^{(k)} = -\int_{-1}^{x_3} \left[\mathbf{L}_2 \left(\mathbf{u}^k - \eta \mathbf{D} u_3^k \right) \right] d\eta - \mathbf{f}^k(x_1, x_2, x_3), \tag{42}$$

$$(1 - \bar{\mu}_1 \partial_{11} - \bar{\mu}_1 \partial_{22}) \sigma_3^{(k)} = \int_{-1}^{x_3} (x_3 - \eta) \mathbf{D}^T \left[\mathbf{L}_2 \left(\mathbf{u}^k - \eta \mathbf{D} u_3^k \right) \right] d\eta - f_{3k}(x_1, x_2, x_3), \tag{43}$$

where

$$\mathbf{u}^k = \left[u_1^k(x_1,x_2) \quad u_2^k(x_1,x_2) \right]^T,$$

$$\varphi_{3k}(x_1,x_2,x_3) = -\int_0^{x_3} \left[\mathbf{L}_1 \mathbf{u}^{(k-1)} - \tilde{c}_{33}^{-1} \left(1 - \bar{\mu}_1 \partial_{11} - \bar{\mu}_1 \partial_{22}\right) \sigma_3^{(k-2)} + (\tilde{c}_{33}^{-1} \bar{\mu}_2 \partial_{33}) \sigma_3^{(k-3)} \right] d\eta,$$

$$\boldsymbol{\varphi}^k = \begin{Bmatrix} \varphi_{1k}(x_1,x_2,,x_3) \\ \varphi_{2k}(x_1,x_2,x_3) \end{Bmatrix} = \int_0^{x_3} \left[\mathbf{S} \left(1 - \bar{\mu}_1 \partial_{11} - \bar{\mu}_1 \partial_{22}\right) \sigma_s^{(k-1)} - \mathbf{S} \left(\bar{\mu}_2 \partial_{33}\right) \sigma_s^{(k-2)} - \mathbf{D} \varphi_{3k} \right] d\eta,$$

$$\mathbf{f}^k = \begin{Bmatrix} f_{1k}\left(x_1,x_2,x_3,\right) \\ f_{2k}\left(x_1,x_2,x_3\right) \end{Bmatrix} = \int_{-1}^{x_3} \left[\mathbf{L}_2 \varphi^k - \left(\bar{\mu}_2 \partial_{333}\right) \sigma_s^{(k-1)} + \mathbf{L}_3 \left(1 - \bar{\mu}_1 \partial_{11} - \bar{\mu}_1 \partial_{22}\right) \sigma_3^{(k-1)} - \mathbf{L}_3 \left(\bar{\mu}_2 \partial_{33}\right) \sigma_3^{(k-2)} \right] d\eta,$$

$$f_{3k}\left(x_1,x_2,x_3\right) = -\int_{-1}^{x_3} \mathbf{D}^T \mathbf{f}^k d\eta.$$

u_3^k and $\mathbf{u}^k$ represent the k^{th}-order modifications to the variables of the displacement components. By imposing the associated lateral boundary conditions (Eq. (29b)) on Eqs. (42) and (43), we again obtain the CPT governing equations, and the non-homogeneous terms can be calculated using the lower-order solution. The resulting equations are obtained, as follows:

$$K_{11} u_1^k + K_{12} u_2^k + K_{13} u_3^k = f_{1k}\left(x_3 = 1\right), \tag{44}$$

$$K_{21} u_1^k + K_{22} u_2^k + K_{23} u_3^k = f_{2k}\left(x_3 = 1\right), \tag{45}$$

$$K_{31} u_1^k + K_{32} u_2^k + K_{33} u_3^k = f_{3k}\left(x_3 = 1\right) + \frac{\partial f_{1k}\left(x_3 = 1\right)}{\partial x_1} + \frac{\partial f_{2k}\left(x_3 = 1\right)}{\partial x_2}. \tag{46}$$

After the asymptotic process, we obtain the edge conditions for the higher-order problems, as follows:

$$u_2^k = 0, u_3^k = 0, N_1^{(\mathrm{k})} = 0 \text{ and } M_1^{(\mathrm{k})} = 0, \text{ at } x_1 = 0 \text{ and } x_1 = L_x/L, \tag{47a}$$

$$u_1^k = 0, u_3^k = 0, N_2^{(\mathrm{k})} = 0 \text{ and } M_2^{(\mathrm{k})} = 0, \text{ at } x_2 = 0 \text{ and } x_2 = L_y/L, \tag{47b}$$

in which $N_i^{(\mathrm{k})} = \int_{-1}^{1} \sigma_i^{(k)} dx_3$, $M_i^{(\mathrm{k})} = \int_{-1}^{1} x_3 \sigma_i^{(k)} dx_3$, and $i = 1$ and 2.

The higher-order modifications of mid-surface displacement components (u_1^k, u_2^k and u_3^k) can be obtained by solving Eqs. (44)–(46) combined with the edge conditions given in Eqs. (47a) and (47b). Once these are determined, the higher-order modifications of displacement components are given by Eqs. (40) and (41), the transverse stresses by Eqs. (42) and (43) and the in-surface stresses by Eq. (28).

Equations (35)–(37) and (44)–(46) show that the differential operators among the various order problems remain identical, and the nonhomogeneous terms of higher-order problems can be calculated from the lower-order solution. The solution process of the leading-order problem can be repeatedly applied to the higher-order problems. The present asymptotic solutions can thus be determined order-by-order in a hierarchical and consistent manner.

6 Applications

6.1 Leading-order solution

The bending problem of simply-supported, single-layered isotropic/orthotropic nanoplates and GSs is studied by using Navier's method, in which the variables of displacement and stress components are expanded as double Fourier series functions in the in-plane directions. For this problem, the governing equations of the leading-order problem can thus be solved by letting

$$u_1^0(x_1, x_2) = \sum_{\hat{m}=1}^{\infty} \sum_{\hat{n}=1}^{\infty} \tilde{u}_{1\hat{m}\hat{n}}^0 \cos\tilde{m}x_1 \sin\tilde{n}x_2, \tag{48}$$

$$u_2^0(x_1, x_2) = \sum_{\hat{m}=1}^{\infty} \sum_{\hat{n}=1}^{\infty} \tilde{u}_{2\hat{m}\hat{n}}^0 \sin\tilde{m}x_1 \cos\tilde{n}x_2, \tag{49}$$

$$u_3^0(x_1, x_2) = \sum_{\hat{m}=1}^{\infty} \sum_{\hat{n}=1}^{\infty} \tilde{u}_{3\hat{m}\hat{n}}^0 \sin\tilde{m}x_1 \sin\tilde{n}x_2, \tag{50}$$

where $\tilde{m} = \hat{m}\pi L/L_x$, $\tilde{n} = \hat{n}\pi L/L_y$, $\hat{m}$ and $\hat{n}$ denote the half-wave numbers, and these are positive integers.

According to Eqs. (48)–(50), the other field variables should be also the forms of double Fourier series functions, such that the simply-supported edge conditions are satisfied, and these are given as

$$\left[u_1^{(0)} \quad \tau_{13}^{(0)}\right] = \sum_{\hat{m}=1}^{\infty} \sum_{\hat{n}=1}^{\infty} \left[\tilde{u}_{1\hat{m}\hat{n}}^{(0)}(x_3) \quad \tilde{\tau}_{13\hat{m}\hat{n}}^{(0)}(x_3)\right] \cos\tilde{m}x_1 \sin\tilde{n}x_2, \tag{51}$$

$$\left[u_2^{(0)} \quad \tau_{23}^{(0)}\right] = \sum_{\hat{m}=1}^{\infty} \sum_{\hat{n}=1}^{\infty} \left[\tilde{u}_{2\hat{m}\hat{n}}^{(0)}(x_3) \quad \tilde{\tau}_{23\hat{m}\hat{n}}^{(0)}(x_3)\right] \sin\tilde{m}x_1 \cos\tilde{n}x_2, \tag{52}$$

$$\left[u_3^{(0)} \;\; \sigma_1^{(0)} \;\; \sigma_2^{(0)} \;\; \sigma_3^{(0)}\right] = \sum_{\hat{m}=1}^{\infty}\sum_{\hat{n}=1}^{\infty}\left[\tilde{u}_{3\hat{m}\hat{n}}^{(0)}(x_3) \;\; \tilde{\sigma}_{1\hat{m}\hat{n}}^{(0)}(x_3) \;\; \tilde{\sigma}_{2\hat{m}\hat{n}}^{(0)}(x_3) \;\; \tilde{\sigma}_{3\hat{m}\hat{n}}^{(0)}(x_3)\right] \sin\tilde{m}x_1 \sin\tilde{n}x_2, \tag{53}$$

$$\left[\tau_{12}^{(0)}\right] = \sum_{\hat{m}=1}^{\infty}\sum_{\hat{n}=1}^{\infty}\left[\tilde{\tau}_{12\hat{m}\hat{n}}^{(0)}(x_3)\right]\cos\tilde{m}x_1 \cos\tilde{n}x_2. \tag{54}$$

The summation sign will not be shown in the following derivation for brevity. Substituting Eqs. (48)–(50) into Eqs. (35)–(37) gives

$$\begin{bmatrix} k_{11} & k_{12} & k_{13} \\ k_{21} & k_{22} & k_{23} \\ k_{31} & k_{32} & k_{33} \end{bmatrix} \begin{Bmatrix} \tilde{u}_{1\hat{m}\hat{n}}^0 \\ \tilde{u}_{2\hat{m}\hat{n}}^0 \\ \tilde{u}_{3\hat{m}\hat{n}}^0 \end{Bmatrix} = \begin{Bmatrix} 0 \\ 0 \\ -\left[1+\bar{\mu}_1\left(\tilde{m}^2+\tilde{n}^2\right)\right]\left(\tilde{q}_{3\hat{m}\hat{n}}^{+}-\tilde{q}_{3\hat{m}\hat{n}}^{-}\right) \end{Bmatrix}, \tag{55}$$

where the applied external loads on the lateral surfaces, $\bar{q}_3^{\pm}(x_1,x_2)$, are expressed as $\bar{q}_3^{\pm}(x_1,x_2) = \sum_{\hat{m}=1}^{\infty}\sum_{\hat{n}=1}^{\infty}\tilde{q}_{3\hat{m}\hat{n}}^{\pm}\sin\tilde{m}x_1\sin\tilde{n}x_2$, and

$$k_{11} = \tilde{m}^2\tilde{A}_{11} + \tilde{n}^2\tilde{A}_{66}, \tag{56a}$$
$$k_{12} = \tilde{m}\,\tilde{n}\,\left(\tilde{A}_{12}+\tilde{A}_{66}\right), \tag{56b}$$
$$k_{13} = -\tilde{m}^3\tilde{B}_{11} - \tilde{m}\,\tilde{n}^2\left(\tilde{B}_{12}+2\tilde{B}_{66}\right), \tag{56c}$$
$$k_{21} = k_{12}, \tag{56d}$$
$$k_{22} = \tilde{m}^2\tilde{A}_{66} + \tilde{n}^2\tilde{A}_{22}, \tag{56e}$$
$$k_{23} = -\tilde{m}^2\,\tilde{n}\left(\tilde{B}_{12}+2\tilde{B}_{66}\right) - \tilde{n}^3\tilde{B}_{22}, \tag{56f}$$
$$k_{31} = k_{13}, \tag{56g}$$
$$k_{32} = k_{23}, \tag{56h}$$
$$k_{33} = \tilde{m}^4\tilde{D}_{11} + \tilde{m}^2\tilde{n}^2\left(2\tilde{D}_{12}+4\tilde{D}_{66}\right) + \tilde{n}^4\tilde{D}_{22}, \tag{56i}$$

In this work, the nanoplates and GSs are considered to be orthotropic or isotropic materials, the material properties of which are symmetric to the mid-plane, such that the coupled extension-bending coefficients ($\tilde{B}_{ij}$) are identical to zero (i.e., $\tilde{B}_{ij} = 0$), which leads to $k_{13} = k_{23} = k_{31} = k_{32} = 0$. The governing equations of in-plane and out-of-plane directions given in Eq. (55) can thus be seperated and solved, as follows:

$$\tilde{u}_{1\hat{m}\hat{n}}^0 = \tilde{u}_{2\hat{m}\hat{n}}^0 = 0, \tag{57}$$

$$\tilde{u}_{3\hat{m}\hat{n}}^0 = -\left[1+\bar{\mu}_1\left(\tilde{m}^2+\tilde{n}^2\right)\right]\left(\tilde{q}_{3\hat{m}\hat{n}}^{+}-\tilde{q}_{3\hat{m}\hat{n}}^{-}\right)/k_{33}. \tag{58}$$

According to Eqs (57) and (58), the through-thickness distributions of various field variables of the leading-order problem can be obtained, as follows:

$$\tilde{u}^{(0)}_{3\hat{m}\hat{n}} = \tilde{u}^{0}_{3\hat{m}\hat{n}}, \tag{59}$$

$$\tilde{\mathbf{u}}^{(0)}_{\hat{m}\hat{n}} = -x_3\tilde{\mathbf{D}}u^{0}_{3\hat{m}\hat{n}}, \tag{60}$$

$$\tilde{\sigma}^{(0)}_{s\hat{m}\hat{n}} = \frac{1}{\left[1+\bar{\mu}_1\left(\tilde{m}^2+\tilde{n}^2\right)\right]}\int_{-1}^{x_3}\tilde{\mathbf{L}}_2\tilde{\mathbf{u}}^{(0)}_{\hat{m}\hat{n}}d\eta, \tag{61}$$

$$\tilde{\sigma}^{(0)}_{3\hat{m}\hat{n}} = \int_{-1}^{x_3}\tilde{\mathbf{D}}^T\tilde{\sigma}^{(0)}_{s\hat{m}\hat{n}}d\eta, \tag{62}$$

$$\tilde{\sigma}^{(0)}_{p\hat{m}\hat{n}} = \frac{1}{\left[1+\bar{\mu}_1\left(\tilde{m}^2+\tilde{n}^2\right)\right]}\tilde{\mathbf{B}}_1\tilde{\mathbf{u}}^{(0)}_{\hat{m}\hat{n}}, \tag{63}$$

where $\tilde{\sigma}^{(0)}_{p\hat{m}\hat{n}}$, $\tilde{\sigma}^{(0)}_{s\hat{m}\hat{n}}$ and $\tilde{\sigma}^{(0)}_{3\hat{m}\hat{n}}$ are the so-called local stress components of the leading-order level, which will be independent of the nonlocal parameter, while $[1+\bar{\mu}_1(\tilde{m}^2+\tilde{n}^2)]\tilde{\sigma}^{(0)}_{p\hat{m}\hat{n}}$, $\left[1+\bar{\mu}_1\left(\tilde{m}^2+\tilde{n}^2\right)\right]\tilde{\sigma}^{(0)}_{s\hat{m}\hat{n}}$ and $\left[1+\bar{\mu}_1\left(\tilde{m}^2+\tilde{n}^2\right)\right]\sigma^{(0)}_{3\hat{m}\hat{n}}$ are the nonlocal stress ones, which will be dependent upon the nonlocal parameter, and

$$\tilde{\mathbf{u}}^{(0)}_{\hat{m}\hat{n}} = \begin{bmatrix}\tilde{u}^{(0)}_{1\hat{m}\hat{n}}\\ \tilde{u}^{(0)}_{2\hat{m}\hat{n}}\end{bmatrix}, \quad \tilde{\sigma}^{(0)}_{p\hat{m}\hat{n}} = \begin{bmatrix}\tilde{\sigma}^{(0)}_{1\hat{m}\hat{n}}\\ \tilde{\sigma}^{(0)}_{2\hat{m}\hat{n}}\\ \tilde{\tau}^{(0)}_{12\hat{m}\hat{n}}\end{bmatrix}, \quad \tilde{\sigma}^{(0)}_{s\hat{m}\hat{n}} = \begin{bmatrix}\tilde{\tau}^{(0)}_{13\hat{m}\hat{n}}\\ \tilde{\tau}^{(0)}_{23\hat{m}\hat{n}}\end{bmatrix}, \quad \tilde{\mathbf{D}} = \begin{bmatrix}\tilde{m}\\ \tilde{n}\end{bmatrix},$$

$$\tilde{\mathbf{L}}_2 = \begin{bmatrix}\left(\tilde{m}^2\tilde{Q}_{11}+\tilde{n}^2\tilde{Q}_{66}\right) & \tilde{m}\tilde{n}\left(\tilde{Q}_{12}+\tilde{Q}_{66}\right)\\ \tilde{m}\tilde{n}\left(\tilde{Q}_{12}+\tilde{Q}_{66}\right) & \tilde{m}^2\tilde{Q}_{66}+\tilde{n}^2\tilde{Q}_{22}\end{bmatrix}, \quad \tilde{\mathbf{B}}_1 = \begin{bmatrix}-\tilde{m}\tilde{Q}_{11} & -\tilde{n}\tilde{Q}_{12}\\ -\tilde{m}\tilde{Q}_{12} & -\tilde{n}\tilde{Q}_{22}\\ \tilde{n}\tilde{Q}_{66} & \tilde{m}\tilde{Q}_{66}\end{bmatrix}.$$

6.2 Higher-order modifications

Carrying out the solution to order $\in^{2k}$ $(k=1,2,\cdots)$, we find that the nonhomogeneous terms $(f_{ik}(x_1,x_2,x_3),\ i=1-3)$ and the relevant functions $(\varphi_{ik}(x_1,x_2,x_3),\ i=1-3)$ in the $\in^{2k}$-order equations are

$$[f_{1k}\ \ \varphi_{1k}] = \sum_{\hat{m}=1}^{\infty}\sum_{\hat{n}=1}^{\infty}\left[\tilde{f}_{1k\hat{m}\hat{n}}(x_3)\ \ \tilde{\varphi}_{1k\hat{m}\hat{n}}(x_3)\right]\cos\tilde{m}x_1\sin\tilde{n}x_2, \tag{64}$$

$$[f_{2k}\ \ \varphi_{2k}] = \sum_{\hat{m}=1}^{\infty}\sum_{\hat{n}=1}^{\infty}\left[\tilde{f}_{2k\hat{m}\hat{n}}(x_3)\ \ \tilde{\varphi}_{2k\hat{m}\hat{n}}(x_3)\right]\sin\tilde{m}x_1\cos\tilde{n}x_2, \tag{65}$$

$$[f_{3k}\ \ \varphi_{3k}] = \sum_{\hat{m}=1}^{\infty}\sum_{\hat{n}=1}^{\infty}\left[\tilde{f}_{3k\hat{m}\hat{n}}(x_3)\ \ \tilde{\varphi}_{3k\hat{m}\hat{n}}(x_3)\right]\sin\tilde{m}x_1\sin\tilde{n}x_2, \tag{66}$$

where $\tilde{f}_{ik\hat{m}\hat{n}}$ and $\tilde{\varphi}_{ik\hat{m}\hat{n}}\,(i=1-3)$ are the relevant coefficients.

The governing equations of the higher-order problems can be solved by letting

$$u_1^k(x_1,\,x_2) = \sum_{\hat{m}=1}^{\infty}\sum_{\hat{n}=1}^{\infty} \tilde{u}_{1\hat{m}\hat{n}}^k \cos\tilde{m}x_1 \ \sin\tilde{n}x_2, \tag{67}$$

$$u_2^k\ (x_1,\,x_2) = \sum_{\hat{m}=1}^{\infty}\sum_{\hat{n}=1}^{\infty} \tilde{u}_{2\hat{m}\hat{n}}^k \sin\tilde{m}x_1 \ \cos\tilde{n}x_2, \tag{68}$$

$$u_3^k(x_1,\,x_2) = \sum_{\hat{m}=1}^{\infty}\sum_{\hat{n}=1}^{\infty} \tilde{u}_{3\hat{m}\hat{n}}^k \sin\tilde{m}x_1 \ \sin\tilde{n}x_2. \tag{69}$$

According to Eqs. (67)–(69), the other field variables of the k^{th}-order problems should be also in the form of double Fourier series functions, such that the simply-supported edge conditions are satisfied, and these are given as

$$\left[u_1^{(k)}\ \ \tau_{13}^{(k)}\right] = \sum_{\hat{m}=1}^{\infty}\sum_{\hat{n}=1}^{\infty}\left[\tilde{u}_{1\hat{m}\hat{n}}^{(k)}(x_3)\ \ \tilde{\tau}_{13\hat{m}\hat{n}}^{(k)}(x_3)\right]\cos\tilde{m}x_1\sin\tilde{n}x_2, \tag{70}$$

$$\left[u_2^{(k)}\ \ \tau_{23}^{(k)}\right] = \sum_{\hat{m}=1}^{\infty}\sum_{\hat{n}=1}^{\infty}\left[\tilde{u}_{2\hat{m}\hat{n}}^{(k)}(x_3)\ \ \tilde{\tau}_{23\hat{m}\hat{n}}^{(k)}(x_3)\right]\sin\tilde{m}x_1\cos\tilde{n}x_2, \tag{71}$$

$$\left[u_3^{(k)}\ \ \sigma_1^{(k)}\ \ \sigma_2^{(k)}\ \ \sigma_3^{(k)}\right] = \sum_{\hat{m}=1}^{\infty}\sum_{\hat{n}=1}^{\infty}\left[\tilde{u}_{3\hat{m}\hat{n}}^{(k)}(x_3)\ \ \tilde{\sigma}_{1\hat{m}\hat{n}}^{(k)}(x_3)\ \ \tilde{\sigma}_{2\hat{m}\hat{n}}^{(k)}(x_3)\ \ \tilde{\sigma}_{3\hat{m}\hat{n}}^{(k)}(x_3)\right] \sin\tilde{m}x_1\sin\tilde{n}x_2, \tag{72}$$

$$\left[\tau_{12}^{(k)}\right] = \sum_{\hat{m}=1}^{\infty}\sum_{\hat{n}=1}^{\infty}\left[\tilde{\tau}_{12\hat{m}\hat{n}}^{(k)}(x_3)\right]\cos\tilde{m}x_1\cos\tilde{n}x_2. \tag{73}$$

The summation sign will not be shown in the following derivation for brevity.

Substituting Eqs. (67)–(69) and Eqs. (64)–(66) into Eqs. (44)–(46) gives

$$\begin{bmatrix} k_{11} & k_{12} & k_{13} \\ k_{21} & k_{22} & k_{23} \\ k_{31} & k_{32} & k_{33} \end{bmatrix} \begin{Bmatrix} \tilde{u}_{1\hat{m}\hat{n}}^k \\ \tilde{u}_{2\hat{m}\hat{n}}^k \\ \tilde{u}_{3\hat{m}\hat{n}}^k \end{Bmatrix} = \begin{Bmatrix} \tilde{f}_{1k\hat{m}\hat{n}}(1) \\ \tilde{f}_{2k\hat{m}\hat{n}}(1) \\ \tilde{f}_{3k\hat{m}\hat{n}}(1) - \tilde{m}\tilde{f}_{1k\hat{m}\hat{n}}(1) - \tilde{n}\tilde{f}_{2k\hat{m}\hat{n}}(1) \end{Bmatrix}, \tag{74}$$

Because $k_{13} = k_{23} = k_{31} = k_{32} = 0$, the mid-plane displacement modifications of the k^{th}-order can be obtained by a matrix partition process, as follows:

$$\begin{Bmatrix} \tilde{u}_{1\hat{m}\hat{n}}^k \\ \tilde{u}_{2\hat{m}\hat{n}}^k \end{Bmatrix} = \begin{bmatrix} k_{11} & k_{12} \\ k_{21} & k_{22} \end{bmatrix}^{-1} \begin{Bmatrix} \tilde{f}_{1k\hat{m}\hat{n}}(1) \\ \tilde{f}_{2k\hat{m}\hat{n}}(1) \end{Bmatrix}, \tag{75}$$

$$\tilde{u}^k_{3\hat{m}\hat{n}} = \left[\tilde{f}_{3k\hat{m}\hat{n}}(1) - \tilde{m}\tilde{f}_{1k\hat{m}\hat{n}}(1) - \tilde{n}\tilde{f}_{2k\hat{m}\hat{n}}(1)\right]/k_{33}. \tag{76}$$

According to Eqs (75) and (76), the through-thickness distributions of various field variables of the k^{th}-order modifications can be obtained, as follows:

$$\tilde{u}^{(k)}_{3\hat{m}\hat{n}} = \tilde{u}^k_{3\hat{m}\hat{n}} + \tilde{\varphi}_{3k\hat{m}\hat{n}}, \tag{77}$$

$$\tilde{\mathbf{u}}^{(k)}_{\hat{m}\hat{n}} = \tilde{\mathbf{u}}^k_{\hat{m}\hat{n}} - x_3\tilde{\mathbf{D}}u^k_{3\hat{m}\hat{n}} + \tilde{\varphi}^k_{\hat{m}\hat{n}}, \tag{78}$$

$$\begin{aligned}\tilde{\sigma}^{(k)}_{s\hat{m}\hat{n}} = {} & \frac{1}{\left[1+\bar{\mu}_1\left(\tilde{m}^2+\tilde{n}^2\right)\right]}\int_{-1}^{x_3}\left\{\tilde{\mathbf{L}}_2\tilde{\mathbf{u}}^{(k)}_{\hat{m}\hat{n}} + \tilde{\mathbf{L}}_3\left[1+\bar{\mu}_1\left(\tilde{m}^2+\tilde{n}^2\right)\right]\tilde{\sigma}^{(k-1)}_{3\hat{m}\hat{n}}\right\}d\eta \\ & + \frac{1}{\left[1+\bar{\mu}_1\left(\tilde{m}^2+\tilde{n}^2\right)\right]}\left\{\bar{\mu}_2\left[\tilde{\sigma}^{(k-1)}_{s\hat{m}\hat{n}},_{33}\right]\Big|^{x_3}_{-1} - \bar{\mu}_2\tilde{\mathbf{L}}_3\left[\tilde{\sigma}^{(k-2)}_{3\hat{m}\hat{n}},_3\right]\Big|^{x_3}_{-1}\right\},\end{aligned} \tag{79}$$

$$\tilde{\sigma}^{(k)}_{3\hat{m}\hat{n}} = \int_{-1}^{x_3}\tilde{\mathbf{D}}^T\tilde{\sigma}^{(k)}_{s\hat{m}\hat{n}}d\eta, \tag{80}$$

$$\begin{aligned}\tilde{\sigma}^{(k)}_{p\hat{m}\hat{n}} = {} & \frac{1}{\left[1+\bar{\mu}_1\left(\tilde{m}^2+\tilde{n}^2\right)\right]}\left\{\tilde{\mathbf{B}}_1\tilde{\mathbf{u}}^{(k)}_{\hat{m}\hat{n}} + \mathbf{B}_2\left[1+\bar{\mu}_1\left(\tilde{m}^2+\tilde{n}^2\right)\right]\tilde{\sigma}^{(k-1)}_{3\hat{m}\hat{n}} + \bar{\mu}_2\tilde{\sigma}^{(k-1)}_{p\hat{m}\hat{n}},_{33}\right. \\ & \left. -\bar{\mu}_2\mathbf{B}_2\tilde{\sigma}^{(k-2)}_{3\hat{m}\hat{n}},_{33}\right\},\end{aligned} \tag{81}$$

where

$$\tilde{\mathbf{u}}^k_{\hat{m}\hat{n}} = \begin{bmatrix}\tilde{u}^k_{1\hat{m}\hat{n}}\\ \tilde{u}^k_{2\hat{m}\hat{n}}\end{bmatrix},\quad \tilde{\mathbf{u}}^{(k)}_{\hat{m}\hat{n}} = \begin{bmatrix}\tilde{u}^{(k)}_{1\hat{m}\hat{n}}\\ \tilde{u}^{(k)}_{2\hat{m}\hat{n}}\end{bmatrix},\quad \tilde{\varphi}^k_{\hat{m}\hat{n}} = \begin{bmatrix}\tilde{\varphi}_{1k\hat{m}\hat{n}}\\ \tilde{\varphi}_{2k\hat{m}\hat{n}}\end{bmatrix},\quad \tilde{\mathbf{L}}_3 = \begin{bmatrix}-\tilde{m}\tilde{c}_{13}\\ -\tilde{n}\tilde{c}_{23}\end{bmatrix},$$

$$\tilde{\sigma}^{(k)}_{s\hat{m}\hat{n}} = \begin{bmatrix}\tilde{\tau}^{(k)}_{13\hat{m}\hat{n}}\\ \tilde{\tau}^{(k)}_{23\hat{m}\hat{n}}\end{bmatrix},\quad \tilde{\sigma}^{(k)}_{p\hat{m}\hat{n}} = \begin{bmatrix}\tilde{\sigma}^{(k)}_{1\hat{m}\hat{n}}\\ \tilde{\sigma}^{(k)}_{2\hat{m}\hat{n}}\\ \tilde{\tau}^{(k)}_{12\hat{m}\hat{n}}\end{bmatrix}.$$

The contributions of the nonlocal parameter (μ) in the in-plane and thickness directions were separated in this dimensionless formulation as $\bar{\mu}_1$ and $\bar{\mu}_2$, respectively, because the thickness dimension is much less than the in-plane one for a nanoplate. In the following numerical examples, we let $\bar{\mu}_1 = \bar{\mu}_2$, the corresponding relations of which in a dimensional form are $\mu_1 = \mu$ and $\mu_2 = \mu$ [4], to reasonably equalize their contributions to the mechanical behaviors of a nanoplate and GSs. In addition, $\mu_1 = \mu$ and $\mu_2 = 0$ are commonly used in the advanced and refined 2D nonlocal plate theories.

7 Illustrative examples

7.1 Single-layered isotropic/orthotropic nanoplates

A benchmark problem with regard to the static analysis of simply-supported, isotropic and orthotropic macroplates under sinusoidally and uniformly distributed loads has been presented by Reddy (2002) using the TSDPT. Reddy's solutions can be used to validate the accuracy and convergence of the 3D nonlocal asymptotic theory in the case of $\mu = 0$. The deviation between the 3D local ($\mu = 0$) and nonlocal ($\mu \neq 0$) asymptotic solutions can also be examined when the dimensions of the plate are reduced to the nanoscale.

Table 1 shows the dimensionless center displacement component ($\bar{u}_z$) induced in single-layered isotropic and orthotropic nanoplates under sinusoidally and uniformly distributed loads on the top surface of the plate, in which $\hat{m} = \hat{n} = 1$ is taken for the single-term sinusoidally distributed load and $\hat{m} = \hat{n} = 1 - 19$ for the uniformly-distributed one. The material properties used in the isotropic and orthotropic cases are $E = 30$ GPa, $\upsilon = 0.3$, and $E_L/E_T = 25$, $G_{LT}/E_T = 0.5$, $G_{TT}/E_T = 0.2$ and $\upsilon_{LT} = \upsilon_{TT} = 0.25$, respectively, in which the subscripts L and T denote the directions parallel and perpendicular to the fiber direction. The geometric parameters of the plate are $L_x = L_y$, $S = L_x/H = 10$ and $H = 1$ nm. The uniform load with intensity q_0 is expressed as the double Fourier series functions, as follows:

$$\bar{q}_0 = \sum_{\hat{m}=1,3,\cdots}^{\infty} \sum_{\hat{n}=1,3,\cdots}^{\infty} \bar{q}_{3\hat{m}\hat{n}} \sin \tilde{m} x_1 \sin \tilde{n} x_2 \tag{82}$$

where $\bar{q}_0 = q_0/(Q \in^3)$ and $\bar{q}_{3\hat{m}\hat{n}} = 16q_0/\left[\left(\pi^2 \hat{m}\hat{n}\right)\left(Q \in^3\right)\right]$.

For comparison purposes, a set of dimensionless forms of nonlocal field variables are defined, as follows:

$$\begin{aligned}
&(\bar{u}_x, \bar{u}_y, \bar{u}_z) = \left[\left(u_x E_2 H^2\right)/\left(q_0 L_x^3\right),\ \left(u_y E_2 H^2\right)/\left(q_0 L_x^3\right),\ -\left(10^2 u_z E_2 H^3\right)/\left(q_0 L_x^4\right)\right], \\
&(\bar{\sigma}_x, \bar{\sigma}_y, \bar{\tau}_{xy}) = \left[H^2/\left(q_0 L_x^2\right)\right]\left(\sigma_x^{nl}, \sigma_y^{nl}, \tau_{xy}^{nl}\right), \\
&(\bar{\tau}_{xz}, \bar{\tau}_{yz}, \bar{\sigma}_z) = \left[\tau_{xz}^{nl} H/(q_0 L_x),\ \ \tau_{yz}^{nl} H/(q_0 L_x),\ \ \sigma_z^{nl}/q_0\right],
\end{aligned} \tag{83}$$

in which $\sigma_x^{nl}, \sigma_y^{nl}, \sigma_z^{nl}, \tau_{xz}^{nl}, \tau_{yz}^{nl}, \tau_{xy}^{nl}$ are the nonlocal stress components, and these can be determined by means of multiplying their local counterparts by a coefficient, $\left[1 + \bar{\mu}_1\left(\tilde{m}^2 + \tilde{n}^2\right)\right]$, for each double Fourier series loading term.

It can be seen in Table 1 that the local ($\mu = 0$) and nonlocal ($\mu \neq 0$) asymptotic solutions converge rapidly. The convergent solutions are obtained at the $\in^4$-order level in the cases of moderately thick nanoplates ($L_x/H = 10$), and the $\in^2$-order

Table 1: The dimensionless center displacement components induced in the single-layer isotropic and orthotropic nanoplates under the sinusoidally and uniformly distributed loads ($L_x = L_y$, $S = L_x/H = 10$, $H = 1$ nm, $\bar{u}_z = -10^2 u_z E_2 H^3/(q_0 L_x^4)$).

Materials	μ	Theories	Sinusoidally distributed load ($\hat{m} = \hat{n} = 1$)				Uniform load ($\hat{m}, \hat{n} = 1 - 19$)			
			$L_x/H = 10$	$L_x/H = 12.5$	$L_x/H = 20$	$L_x/H = 100$	$L_x/H = 10$	$L_x/H = 12.5$	$L_x/H = 20$	$L_x/H = 100$
Isotropic	0	Present $\in^0$	2.8026	2.8026	2.8026	2.8026	4.4361	4.4361	4.4361	4.4361
		Present $\in^2$	2.9429	2.8924	2.8377	2.804	4.64	4.5666	4.4871	4.4381
		Present $\in^4$	2.9425	2.8922	2.8377	2.804	4.6396	4.5665	4.487	4.4381
		Present $\in^6$	2.9425	2.8922	2.8377	2.804	4.6396	4.5665	4.487	4.4381
		TSDT (Reddy, 2002)	2.9607	2.9038	2.8422	2.8042	4.666	4.5832	4.4936	4.4438
		CPT (Reddy, 2002)	2.8027	2.8027	2.8027	2.8027	4.4436	4.4436	4.4436	4.4436
	1	Present $\in^0$	3.3558	3.1567	2.9409	2.8081	5.2404	4.9508	4.6372	4.4441
		Present $\in^2$	3.5238	3.2578	2.9777	2.8096	5.4703	5.092	4.6898	4.4462
		Present $\in^4$	3.5233	3.2576	2.9777	2.8096	5.4709	5.0921	4.6898	4.4462
		Present $\in^6$	3.5233	3.2576	2.9777	2.8096	5.4711	5.0921	4.6898	4.4462
	2	Present $\in^0$	3.909	3.5107	3.0792	2.8137	6.0447	5.4656	4.8382	4.4522
		Present $\in^2$	4.1047	3.6232	3.1178	2.8151	6.3006	5.6174	4.8925	4.4542
		Present $\in^4$	4.1041	3.623	3.1177	2.8151	6.3022	5.6178	4.8925	4.4542
		Present $\in^6$	4.1041	3.623	3.1177	2.8151	6.3025	5.6178	4.8925	4.4542
Orthotropic	0	Present $\in^0$	0.4312	0.4312	0.4312	0.4312	0.6497	0.6497	0.6497	0.6497
		Present $\in^2$	0.6395	0.5646	0.4833	0.4333	0.9546	0.8448	0.7259	0.6528
		Present $\in^4$	0.6344	0.5624	0.483	0.4333	0.9474	0.8419	0.7255	0.6528
		Present $\in^6$	0.6348	0.5626	0.483	0.4333	0.9467	0.8417	0.7255	0.6528
		TSDT (Reddy, 2002)	0.6383	0.5644	0.4836	0.4334	0.9519	0.8442	0.7262	0.6528
		CPT (Reddy, 2002)	0.4313	0.4313	0.4313	0.4313	0.6497	0.6497	0.6497	0.6497
	1	Present $\in^0$	0.5164	0.4857	0.4525	0.4321	0.7453	0.7109	0.6736	0.6507
		Present $\in^2$	0.7658	0.6359	0.5072	0.4342	1.0902	0.9224	0.7523	0.6537
		Present $\in^4$	0.7596	0.6335	0.5068	0.4342	1.085	0.92	0.7519	0.6537
		Present $\in^6$	0.7601	0.6336	0.5068	0.4342	1.0588	0.9155	0.7518	0.6537
	2	Present $\in^0$	0.6015	0.5402	0.4738	0.4329	0.8408	0.772	0.6975	0.6516
		Present $\in^2$	0.892	0.7072	0.531	0.435	1.2258	0.9999	0.7787	0.6547
		Present $\in^4$	0.8848	0.7045	0.5307	0.435	1.2227	0.9981	0.7783	0.6547
		Present $\in^6$	0.8854	0.7047	0.5307	0.435	1.1708	0.9893	0.7781	0.6547

level in the cases of thin nanoplates ($L_x/H > 20$). The convergent local asymptotic solutions closely agree with the ones obtained by using the local TSDPT, and the deviation between these decreases when the nanoplate becomes thinner. The center displacement in the z direction increases when the value of the nonlocal parameter (μ) becomes greater, which means the small length scale effect will soften the gross stiffness of the nanoplate. The increases in the cases of the moderately thick

nanoplates ($L_x/H = 10$) are up to about 20% and 40% for $\mu = 1\text{nm}^2$ and $\mu = 2\text{nm}^2$, respectively, and these reduce to about 5% , 10% and 0.2% and 0.4% in the cases of thin ($L_x/H = 20$) and very thin ($L_x/H = 100$) nanoplates. The small length scale effect on the static behaviors of the nanoplate is significant when the nanoplate becomes thicker.

Figure 2 shows the convergence of the center displacement in the z direction of the isotropic nanoplate with respect to the total number of terms of the double Fourier series functions used to expand the external uniform loads, in which $\in^6$-order solutions are presented with $\hat{m} = \hat{n} = 1-13, 1-15, 1-17$ and $1-19$; $L_x = L_y$, $S = L_x/H = 10$, $H = 1$ nm and $\mu = 2\text{nm}^2$. As expected, using $\hat{m} = \hat{n} = 1-19$ in the numerical examples will lead to the convergent solutions, and this approach has been commonly adopted in the published literature [Reddy (2002)], and was used to obtain the convergent solutions shown in Table 1.

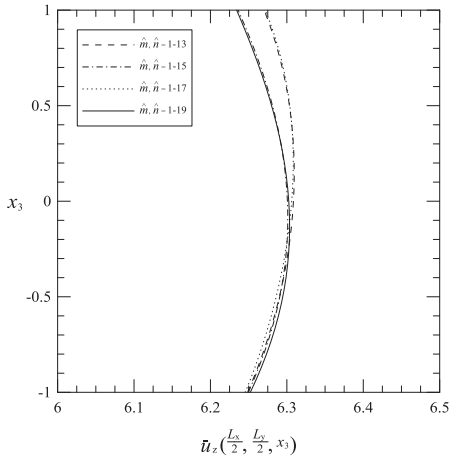

Figure 2: $\in^6$-order solutions of the out-of-plane displacement induced in an isotropic nanoplate under the uniform load, which were expanded with respect to the different total number of terms of double Fourier series functions.

Figure 3 shows the asymptotic solutions of assorted nonlocal field variables induced in the single-layered, orthotropic material nanoplates subjected to a sinusoidally distributed load, $\bar{q}_z = q_0 \sin(\pi x/L_x) \sin(\pi y/L_y)$, in which $L_x = L_y$, $S = L_x/H = 10$, $H = 1$ nm and $\mu = 2$ nm^2. It can be seen that the convergence rates of the nonlocal stress and in-plane displacement components are faster than that of the out-of-plane displacement. The tendency of the through-thickness distribution functions of various field variables induced in these nanoplates ($\mu = 2$ nm^2) are similar to those in the macroplates, which are well-known to be approximate linear functions for the

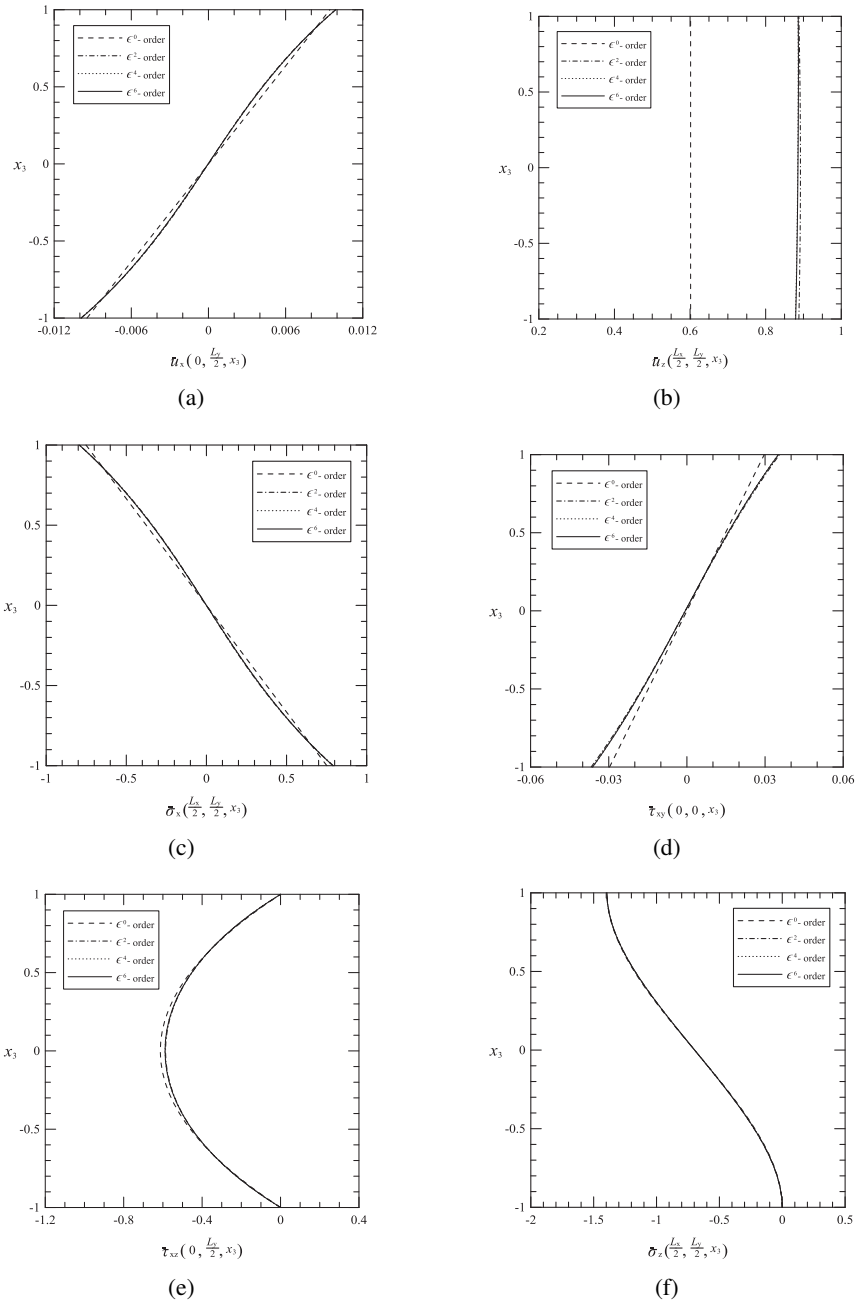

Figure 3: The through-thickness distributions of assorted nonlocal field variables for various orders induced in an orthotropic nanoplate under the sinusoidally distributed loads.

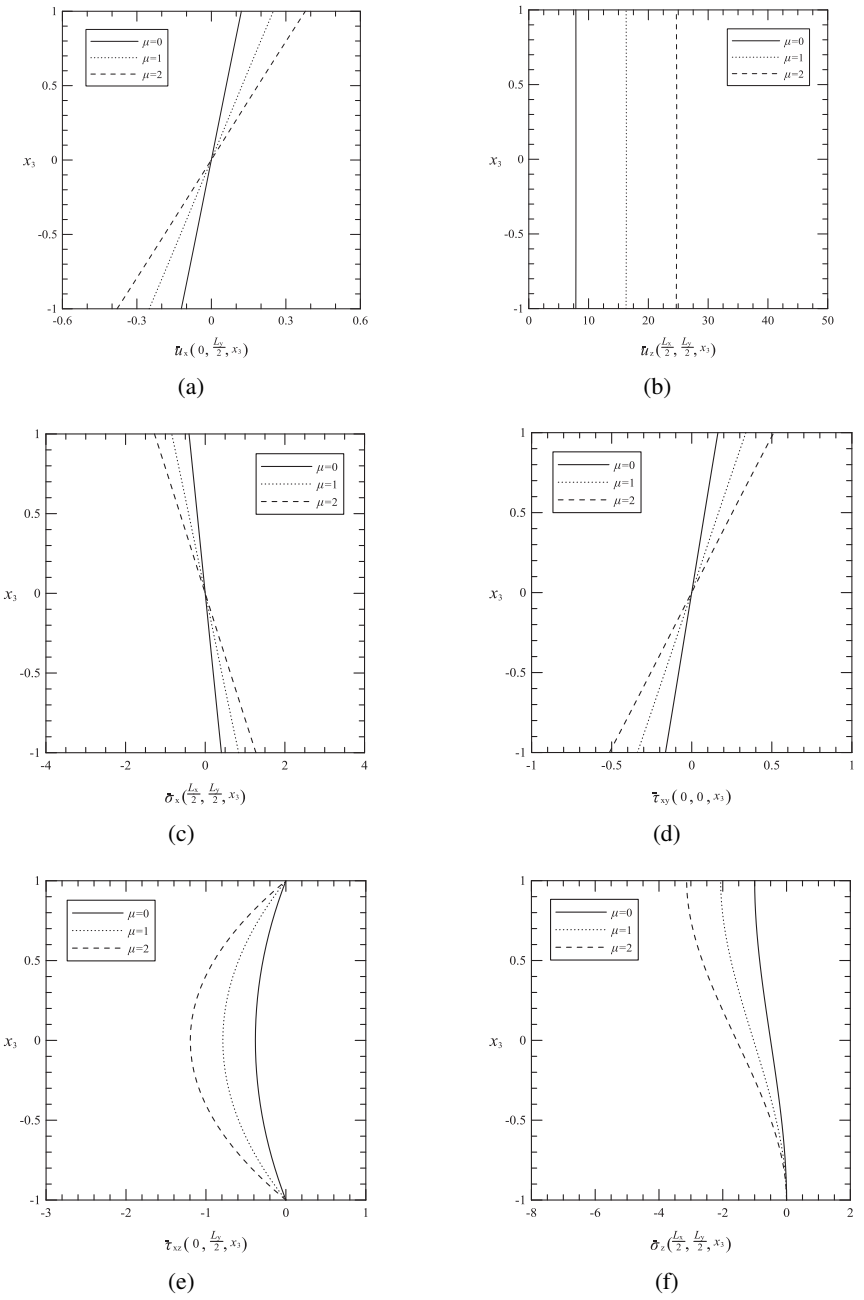

Figure 4: $\in^6$-order solutions for the through-thickness distributions of assorted nonlocal field variables induced in an isotropic GS under the sinusoidally distributed loads and with different values of the nonlocal parameter.

in-plane stress and displacement components, parabolic functions for the transverse shear stress components, and higher-order polynomial functions for the transverse normal stress ones.

7.2 Single-layered isotropic GSs

In this section, we examine the static behaviors of simply-supported, single-layered isotropic square and rectangular GSs, subjected to the mechanical loads. The material properties and thickness of the single-layered GSs were given as $E = 1.02$ TPa, $\upsilon = 0.16$ and $H = 0.34$ nm. Table 2 shows the convergent solutions (i.e. $\in^6$-order ones) of nonlocal displacement and stress components at the crucial positions of the square and rectangular GSs with different aspect ratios and nonlocal parameters (μ), in which a one-term double Fourier series function load ($\hat{m} = \hat{n} = 1$) is applied. It can be seen in Table 2 that the nonlocal displacement and stress components increase when the nonlocal parameter becomes greater. By converting the dimensionless field variables to their corresponding dimensional forms, we found that the magnitude ratios between the out-of- and in-plane displacements induced

Table 2: The convergent solutions (i.e., $\in^6$-order ones) of nonlocal displacement and stress components at the crucial positions of the single-layered graphene sheets with different aspect ratios and nonlocal parameters, and subjected to a sinusoidally distributed load ($H = 0.34$ nm).

L_y/L_x	L_x/H	μ	$\bar{u}_x\left(0, \frac{L_y}{2}, h\right)$	$\bar{u}_z\left(\frac{L_x}{2}, \frac{L_y}{2}, 0\right)$	$\bar{\sigma}_x\left(\frac{L_x}{2}, \frac{L_y}{2}, -h\right)$	$\bar{\sigma}_y\left(\frac{L_x}{2}, \frac{L_y}{2}, -h\right)$	$\bar{\tau}_{yz}\left(\frac{L_x}{2}, 0, 0\right)$	$\bar{\tau}_{xz}\left(0, \frac{L_y}{2}, 0\right)$	$\bar{\tau}_{xy}(0, 0, -h)$
1	10	0	0.0472	3.1331	0.1774	0.1774	−0.2383	−0.2383	−0.1285
		0.5	0.0874	5.8081	0.3289	0.3289	−0.4418	−0.4418	−0.2382
		1	0.1277	8.483	0.4804	0.4804	−0.6453	−0.6453	−0.3479
		1.5	0.168	11.158	0.6319	0.6319	−0.8488	−0.8488	−0.4575
		2	0.2083	13.833	0.7833	0.7833	−1.0523	−1.0523	−0.5672
	20	0	0.0471	3.0341	0.1766	0.1766	−0.2386	−0.2386	−0.1279
		0.5	0.0572	3.6817	0.2143	0.2143	−0.2896	−0.2896	−0.1552
		1	0.0673	4.3293	0.252	0.252	−0.3405	−0.3405	−0.1825
		1.5	0.0773	4.9769	0.2897	0.2897	−0.3914	−0.3914	−0.2098
		2	0.0874	5.6245	0.3274	0.3274	−0.4424	−0.4424	−0.237
	100	0	0.0471	3.0023	0.1763	0.1763	−0.2387	−0.2387	−0.1277
		0.5	0.0475	3.0279	0.1778	0.1778	−0.2408	−0.2408	−0.1288
		1	0.0479	3.0535	0.1793	0.1793	−0.2428	−0.2428	−0.1299
		1.5	0.0483	3.0792	0.1808	0.1808	−0.2448	−0.2448	−0.1309
		2	0.0487	3.1048	0.1823	0.1823	−0.2469	−0.2469	−0.132
2	10	0	0.1207	7.8941	0.4063	0.1602	−0.1908	−0.3816	−0.1641
		0.5	0.1851	12.1065	0.6231	0.2456	−0.2926	−0.5852	−0.2516
		1	0.2495	16.3189	0.8398	0.3311	−0.3944	−0.7888	−0.3392
		1.5	0.314	20.5313	1.0566	0.4166	−0.4962	−0.9924	−0.4267
		2	0.3784	24.7436	1.2734	0.502	−0.598	−1.196	−0.5143
	20	0	0.1207	7.7354	0.4051	0.1597	−0.1909	−0.3819	−0.1636
		0.5	0.1368	8.7674	0.4591	0.181	−0.2164	−0.4328	−0.1854
		1	0.1529	9.7993	0.5131	0.2023	−0.2419	−0.4838	−0.2072
		1.5	0.169	10.8312	0.5672	0.2236	−0.2674	−0.5347	−0.229
		2	0.1851	11.8631	0.6212	0.2449	−0.2928	−0.5856	−0.2509
	100	0	0.1207	7.6846	0.4047	0.1595	−0.191	−0.382	−0.1634
		0.5	0.1213	7.7256	0.4068	0.1604	−0.192	−0.384	−0.1643
		1	0.122	7.7666	0.409	0.1612	−0.193	−0.386	−0.1652
		1.5	0.1226	7.8076	0.4111	0.1621	−0.194	−0.3881	−0.166
		2	0.1233	7.8486	0.4133	0.1629	−0.1951	−0.3901	−0.1669

in the square GSs are about 6.6, 12.9 and 63.8 in the cases of moderately thick ($L_x/H = 10$), thin ($L_x/H = 20$) and very thin ($L_x/H = 100$) plates, respectively, and these ratios between the in-plane stress and transverse shear stress components are about 7.4, 14.8 and 73.8. The magnitude ratios between the out-of-plane and in-plane displacements, as well as the in-plane stress and transverse shear stresses, are significant for very thin GSs, while the ratios will decrease when the GS becomes thicker. In addition, these ratios remain almost unchanged for the rectangular GSs ($L_y/L_x = 2$) with different values of nonlocal parameters.

Figure 4 shows the through-thickness distributions of assorted local and nonlocal field variables induced in the rectangular GSs, in which $L_y/L_x = 2$, $L_x/H = 10$, $\bar{q}_z = q_0 \sin(\pi x/L_x)\sin(\pi y/L_y)$, and $\mu = 0$, 1 and 2 nm^2. It can be seen in Fig. 4 that the nonlocal displacement and stress components are always larger than their corresponding local ones, and that these will increase when the value of the nonlocal parameter becomes greater.

8 Conclusions

In this work we first reformulate the 3D elasticity theory for the static analysis of simply-supported, single-layered isotropic and orthotropic nanoplates and isotropic GSs by using the ENET and perturbation method. A 3D nonlocal elastic problem is asymptotically expanded as a series of 2D nonlocal plate problems, in which the governing equations for various order problems remain the same as those of the nonlocal CPT, although with different nonhomogeneous terms, which can be determined by the lower-order solutions. The 3D nonlocal asymptotic theory can be reduced to its local counterpart by vanishing the nonlocal parameter (i.e., $\mu = 0$). The implementation of this 3D nonlocal asymptotic theory in the numerical examples shows the present asymptotic solutions converge rapidly. The convergent solutions are obtained at the $\in^4$-order level in the cases of moderately thick nanoplates ($L_x/H = 10$), and the $\in^2$-order level in the cases of thin nanoplates ($L_x/H > 20$). The convergent asymptotic solutions agree closely with the corresponding accurate solutions in the cases of macroplates available in the literature, and those of nanoplates and GSs can serve as a standard for assessing the performance of various 2D advanced and refined theories for nanoplates and GSs. In addition, the results show the nonlocal displacement and stress components will increase when the value of the nonlocal parameters become greater.

Acknowledgement: This work was supported by the Ministry of Science and Technology of the Republic of China through Grant MOST 103-2221-E-006-064-MY3.

References

Aghababaei, R.; Reddy, J. N. (2009): Nonlocal third-order shear deformation plate theory with application to bending and vibration of plates. *Journal of Sound and Vibration*, vol. 326, pp. 277–289.

Alibeigloo, A. (2011): Free vibration analysis of nano-plate using three-dimensional theory of elasticity. *Acta Mechanica*, vol. 222, pp. 149–159.

Alibeigloo, A. (2012): Three-dimensional free vibration analysis of multilayered graphene sheets embedded in elastic matrix. *Journal of Vibration and Control*, vol. 19, pp. 2357–2371.

Alibeigloo, A.; Zanoosi, A. A. P. (2013): Static analysis of rectangular nano-plate using three-dimensional theory of elasticity. *Apply Mathematical Modelling*, vol. 37, pp. 7016–7026.

Alzahrani, E. O.; Zenkour, A. M.; Sobhy, M. (2013): Small scale effect on hygro-thermo-mechanical bending of nanoplates embedded in an elastic medium. *Composite Structures*, vol. 105, pp. 163–172.

Ansari, R.; Shojaei, M. F.; Shahabodini, A.; Bazdid-Vahdati, M. (2015): Three-dimensional bending and vibration analysis of functionally graded nanoplates by a novel differential quadrature-based approach. *Composite Structures*, vol. 131, pp. 753–764.

Arani, A. G.; Jalaei, M. H. (2015): Nonlocal dynamic response of embedded single-layered graphene sheet via analytical approach. *Journal of Engineering Mathematics*, doi: 10.1007/s10665-015-9814-x.

Arash, B.; Wang Q. (2012): A review on the application of nonlocal elastic models in modeling of carbon nanotubes and graphenes. *Computational Materials Science*, vol. 51, pp. 303–313.

Brischetto, S. (2014): A continuum elastic three-dimensional model for natural frequencies of single-walled carbon nanotubes. *Composites Part B-Engineering*, vol. 61, pp. 222–228.

Brischetto, S.; Carrera, E. (2012a): Classical and refined shell models for the analysis of nano-reinforced structures. *International Journal of Mechanical Sciences*, vol. 55, pp. 104–117.

Brischetto, S.; Carrera, E. (2012b): Analysis of nano-reinforced layered plates via classical and refined two-dimensional theories. *Multidiscipline Modeling in Materials and Structures*, vol. 8, pp. 4–31.

Brischetto, S.; Tornabene, F.; Fantuzzi, N.; Bacciocchi, M. (2015): Refined 2D and exact 3D shell models for the free vibration analysis of single- and double-walled carbon nanotubes. *Technologies*, vol. 3, pp. 259–284.

Coleman, J. N.; Khan, U.; Blau, W. J.; Gun'ko, Y. K. (2006): Small but strong: a review of the mechanical properties of carbon nanotube-polymer composites. *Carbon*, vol. 44, pp. 1624–1652.

Duan, W. H.; Wang, C. M. (2007): Exact solutions for axisymmetric bending of micro/nanoscale circular plates based on nonlocal plate theory. *Nanotechnology*, vol. 18, pp. 385704.

Eringen, A. C. (1972): Nonlocal polar elastic continua. *International Journal of Engineering Science*, vol. 10, pp. 1–16.

Eringen, A. C. (2002): *Nonlocal Continuum Field Theories*. Springer-Verlag, New York.

Eringen, A. C.; Edelen, D. G. B. (1972): On nonlocal elasticity. *International Journal of Engineering Science*, vol. 10, pp. 233–248.

Esawi, A. M. K.; Farag, M. M. (2007): Carbon nanotube reinforced composites: potential and current challenges. *Materials & Design*, vol. 28, pp. 2394–2401.

Ghavanloo, E.; Fazelzadeh, S. A. (2013): Nonlocal elasticity theory for radial vibration of nanoscale spherical shells. *European Journal of Mechanics A-Solids*, vol. 41, pp. 37–42.

Hosseini-Hashemi, S.; Kermajani, M.; Nazemnezhad, R. (2015): An analytical study on the buckling and free vibration of rectangular nanoplates using nonlocal third-order shear deformation plate theory. *European Journal of Mechanics A-Solids*, vol. 51, pp. 29–43.

Iijima, S. (1991): Helical microtubules of graphitic carbon. *Nature*, vol. 354, pp. 56–58.

Kitipornchai, S.; He, X. Q.; Liew, K. M. (2005): Continuum model for the vibration of multilayered graphene sheets. *Physical Review B-Condensed Matter and Materials Physics*, vol. 72, 075443.

Li, C.; Thostenson, E. T.; Chou, T. W. (2008): Sensors and actuators based on carbon nanotubes and their composites: a review. *Composites Science and Technology*, vol. 68, pp. 1227–1249.

Li, Y. S.; Pan, E. (2016): Bending of a sinusoidal piezoelectric nanoplate with surface effect. *Composite Structures*, vol. 136, pp. 45–55.

Liew, K. M.; He, X. Q.; Kitipornchai, S. (2006): Predicting nanovibration of multi-layered graphene sheets embedded in an elastic matrix. *Acta Materialia*, vol. 54, pp. 4229–4236.

Liew, K. M.; Lei, Z. X.; Zhang, L. W. (2015): Mechanical analysis of functionally graded carbon nanotube reinforced composites: a review. *Composite Structures*, vol. 120, pp. 90–97.

Nayfeh, A. H. (1993): *Introduction to Perturbation Techniques*, John Wiley & Sons, New York.

Novoselov, K. S.; Geim, A. K.; Morozov, S. V.; Jiang, D.; Zhang, Y.; Dubonos, S. V.; Grigorieva, I. V.; Firsov, A. A. (2004): Electric field effect in atomically thin carbon films. *Science*, vol. 306, pp. 666–669.

Pradhan, S. C.; Kumar, A. (2011): Vibration analysis of orthotropic graphene sheets using nonlocal elasticity theory and differential quadrature method. *Composite Structures*, vol. 93, pp. 774–779.

Pradhan, S. C.; Phadikar, J. K. (2009): Nonlocal elasticity theory for vibration of nanoplates. *Journal of Sound and Vibration*, vol. 325, pp. 206–223.

Ramaratnam, A.; Jalili, N. (2006): Reinforcement of piezoelectric polymers with carbon nanotubes: pathway to next-generation sensors. *Journal of Intelligent Material Systems and Structures*, vol. 17, pp. 199–208.

Reddy, J. N. (1984): A refined nonlinear theory of plates with transverse shear deformation. *International Journal of Solids and Structures*, vol. 20, pp. 881–896.

Reddy, J. N. (2002): *Energy and Variational Methods in Applied Mechanics*, John Wiley & Sons, New York.

Reddy, J. N. (2010): Nonlocal nonlinear formulations for bending of classical and shear deformation theories of beams and plates. *International Journal of Engineering Science*, vol. 48, pp. 1507–1518.

Reddy, J. N.; Phan, N. D. (1985): Stability and vibration of isotropic, orthotropic and laminated plates according to a higher-order shear deformation theory. *Journal of Sound and Vibration*, vol. 98, pp. 157–170.

Shen, L.; Shen, H. S.; Zhang, C. L. (2010): Nonlocal plate model for nonlinear vibration of single layer graphene sheets in thermal environments. *Computational Materials Science*, vol. 48, pp. 680–685.

Thai, H. T. (2012): A nonlocal beam theory for bending, buckling, and vibration of nanobeams. *International Journal of Engineering Science*, vol. 52, pp. 56–64.

Thai, H. T.; Vo, T.P. (2012): A nonlocal sinusoidal shear deformation beam theory with application to bending, buckling, and vibration of nanobeams. *International Journal of Engineering Science*, vol. 54, pp. 58–66.

Thai, H. T.; Vo, T. P.; Nguyen, T. K.; Lee, J. (2014): A nonlocal sinusoidal plate model for micro/nanoscale plates. *Proceedings of the institution of mechanical Engineers, Part C: Journal of Mechanical Engineering Science*, vol. 228, pp. 2652–2660.

Wang, Q. (2004): Effective in-plane stiffness and bending rigidity of armchair and zigzag carbon nanotubes. *International Journal of Solids and Structures*, vol. 41, pp. 5451–5461.

Wang, Q. (2005): Wave propagation in carbon nanotubes via nonlocal continuum mechanics. *Journal of Applied Physics*, vol. 98, 124301.

Wang, Q.; Liew, K. M. (2008): Molecular mechanics modeling for properties of carbon nanotubes. *Journal of Applied Physics*, vol. 103, 046103.

Wang, Y. Z.; Li, F. M. (2012): Static bending behaviors of nanoplate embedded in elastic matrix with small scale effects. *Mechanics Research Communications*, vol. 41, pp. 44–48.

Wang, Q.; Wang, C. M. (2007): The constitutive relation and small scale parameter of nonlocal continuum mechanics for modelling carbon nanotubes. *Nanotechnology*, vol. 18, 075702.

Wen, P. H.; Huang, X. J.; Aliabadi, M. H. (2013): Two-dimensional nonlocal elasticity analysis by local integral equation method. *CMES-Computer Modeling in Engineering & Sciences*, vol. 96, pp. 199–225.

Wu, C. P.; Chiu, S. J. (2002): Thermally induced dynamic instability of laminated composite conical shells. *International Journal of Solids and Structures*, vol. 39, pp. 3001–3021.

Wu, C. P.; Chiu, K. H.; Wang, Y. M. (2008): A review on the three-dimensional analytical approaches of multilayered and functionally graded piezoelectric plates and shells. *CMC-Computers, Materials, & Continua*, vol. 8, pp. 93–132.

Wu, C. P.; Syu, Y. S. (2007): Exact solutions of functionally graded piezoelectric shells under cylindrical bending. *International Journal of Solids and Structures*, vol. 44, pp. 6450–6472.

Wu, C. P.; Tarn, J.Q.; Chi, S.M. (1996a): Three-dimensional analysis of doubly curved laminated shells. *Journal of Engineering Mechanics*, vol. 122, pp. 391–401.

Wu, C. P.; Tarn, J. Q.; Chi, S. M. (1996b): An asymptotic theory for dynamic response of doubly curved laminated shells. *International Journal of Solids and Structures*, vol. 33, pp. 3813–3841.

Wu, C. P.; Tarn, J. Q.; Chen, P. Y. (1997): Refined asymptotic theory of doubly curved laminated shells. *Journal of Engineering Mechanics*, vol. 123, pp. 1238–1246.

Wu, C. P.; Tsai, Y. H. (2004): Asymptotic DQ solutions of functionally graded annular spherical shells. *European Journal of Mechanics A-Solids*, vol. 23, pp. 283–299.

Zenkour, A. M.; Sobhy, M. (2013): Nonlocal elasticity theory for thermal buckling of nanoplates lying on Winkler-Pasternak elastic substrate medium. *Physica E-Low-Dimensional Systems & Nanostructures*, vol. 53, pp. 251–259.